New Methods For Approximating Acoustic Wave Transmission Through Ducts

Tamsin Lee

August 21, 2007

Acknowledgments

Firstly, I'd like to thank EPSRC for their generous grant, thus making it possible for me to study this course. Furthermore, a big thank you to all the maths staff, especially Sue, for all their reassurance, as well as all the friends I've made on this course who have helped me and encouraged me to continue working hard, and to all the friends outside of this course who have ensured I don't work too hard. I'd also like to thank my family for their support and Mark for enduring many of my stressed moments throughout this past year. Last, but definitely not least, I'd like to give a special thanks to my supervisors, Peter Chamberlain and Nick Biggs for their endless generosity with their time and patience.

Declaration

I confirm that this is my own work and the use of all material from other sources have been properly and fully acknowledged.

Abstract

This dissertation looks at methods used to model wave scattering over an uneven water bed, namely the mild-slope equation and the modified mild-slope equation. These methods are then manipulated so they can be applied to acoustic wave motion through a duct. The ducts modelled in this dissertation have an undulating region with two uniform regions either side that may or may not have the same width. The walls of the ducts have Dirichlet boundary conditions, however the effect of Neumann boundary conditions are discussed. Both the scattering problem and the trapped wave problem are considered. The scattering problem is modelled with both a single mode approximation and a multi-mode approximation. The results from these two methods are compared. When modelling the trapped wave problem, only the single mode is considered. Nonetheless, the multi-mode approximation applied to this problem is discussed. The occurrence of more than one trapped wave within the undulating region of the duct is also investigated.

Contents

List of Figures

Chapter 1

Introduction

This dissertation explores new methods for approximating acoustic wave motion through a varying duct. An application of the work covered in this dissertation is controlling noise reduction in inlets and exhausts of jet engines, which effectively function like acoustic waveguides.

We will be looking at a cross section of a duct with two regions of constant, but not necessarily the same, width. Joining these two segments will be a region of length ℓ that has varying width.
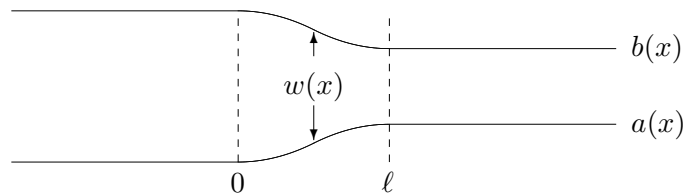
Within the segment of varying width ($0 < x < \ell$), the velocity potential ϕ is modelled using Helmholtz equation, $\nabla^2\phi + k^2\phi = 0$.

With this problem, the boundary conditions on the duct walls remain to be specified. This dissertation will consider Dirichlet boundary conditions on both of these boundaries, meaning $y(a) = y(b) = 0$; other boundary conditions are discussed in the penultimate chapter.

To start, we dedicate a chapter to modelling wave scattering over an uneven water bed, looking specifically at using the mild-slope equation, and its variant, the modified mild-slope equation as approximation methods. Although

1

there are differences between the water bed problem and our acoustic problem, we can develop a model to solve our problem based on methods used to solve the former problem.

In Chapter 2, the reader is introduced to the scattering problem over an uneven water bed. Due to the linearity of the problem, the relation between the amplitudes of the incoming waves and outgoing waves are discovered. Once the scattering problem is defined, we are shown one approach used to acquire the modified mild-slope equation and the mild slope equation. Following the derivation of these equations is a discussion about their use as an approximation tool for a varying water bed model, taking into account the assumptions that are made when they are used. The reader is informed of different developments that have occurred to overcome deficiencies in the mild-slope equation, specifically on multi-mode approximations which ensure the accuracy of the approximation is known.

Now that we are armed with a method of approximation, the next chapter looks at single mode approximations for acoustic wave transmission through a duct. This chapter looks at both the scattering problem and the trapped wave problem. An ordinary differential equation is derived in a similar fashion to the modified mild-slope equation in Chapter 2. This ordinary differential equation is part of a boundary value problem, where the boundary conditions are calculated from the solution in regions of constant width. The boundary conditions for the scattering problem and the trapped problem are different as we'd expect different wave activity in the uniform regions. Also, with the trapped wave problem the conditions for a trapped wave to exist need to be established, therefore it is as an eigenvalue problem.

Chapter 4 investigates the scattering problem when more modes are included. So we return to deriving an ordinary differential to approximate the undulating region. However, this time we find that we N ordinary differential equations, with $2N$ boundary conditions, where N is the number of modes included in the approximation. We calculate the coefficients of the ordinary differential equations and present them as matrices to keep the notation straightforward. The system of boundary value problems is then solved numerically. The results, along with the single mode approximations, are presented and discussed in Chapter 5.

Finally, we finish this dissertation with a summary and details about

further work with acoustic wave transmission through ducts. Areas of further work include multi-mode approximations for the trapped wave problem and discussing the effect of Neumann boundary conditions along the duct walls.

Chapter 2

Wave Scattering Over Uneven Depth

2.1 Introduction

There has been extensive research into water waves propagating over a varying bed. This has resulted in many published papers stating different methods for approximating the solution to this situation.

This dissertation is going to use some of these same methods to approximate acoustic wave transmission through a duct with varying side-walls. So firstly, we shall discuss linear approximations to wave scattering by an uneven bed, focusing on how the mild-slope equation and modified mild-slope equation are used to approximate the full linear solution.

2.2 Defining a Scattering Problem

Let us begin by looking at some aspects of the scattering of a train of plane harmonic waves by variations in the bed, on the basis of linearised theory.

The boundary value problem for the time-independent velocity potential $\phi(x, y, z)$ arising in the three-dimensional case is

$$
\begin{aligned}
\nabla^2 \phi &= 0 & (-h < z < 0) & \quad (2.1) \\
\phi_z - \sigma \phi &= 0 & (z = 0) & \quad (2.2) \\
\phi_z + \nabla_h h . \nabla_h \phi &= 0 & (z = -h) & \quad (2.3)
\end{aligned}
$$

together with the appropriate radiation conditions, where we have used the notation $\nabla_h = \left(\frac{\partial}{\partial x}, \frac{\partial}{\partial y}\right)$ and $\sigma = \frac{\omega^2}{g}$. Here, ω is the prescribed angular wave frequency, g is the gravitational acceleration, and x and z are Cartesian coordinates, with $z = 0$ coinciding with the undisturbed free surface. The surface elevation, which may be regarded as the principal unknown function, is recovered from ϕ by

$$\eta(x, y, t) = \mathrm{Re}\left(\frac{g}{i\omega}\phi(x, y, 0)e^{i\omega t}\right). \tag{2.4}$$

It is assumed that the quiescent depth $h(x, y)$ is a given, bounded function; we shall usually suppose that it is continuous.

Suppose we take a cross-section of the water bed, we then reduce the problem to a two dimensional situation - one for which plane waves propagate in a direction parallel to the x-axis and $h = h(x)$ so that $\phi = \phi(x, z)$, as shown below.

Mixed boundary condition

$\phi_z - \sigma\phi = 0$

$\nabla^2\phi = 0$

z

x

$h(x)$

$\phi_z + \nabla_h h.\nabla_h\phi = 0$

Neumann boundary condition
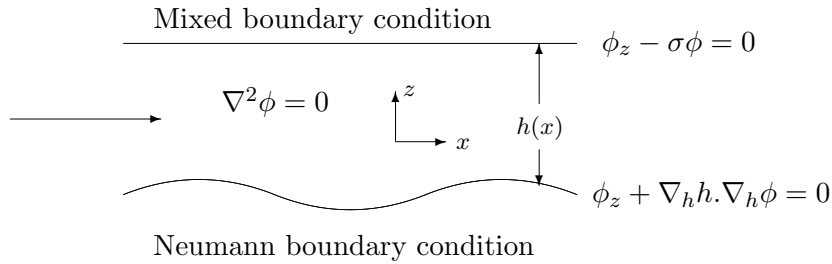
On an interval where h is constant, separation of variables used in the boundary value problem gives

$$\phi(x, z) = \left(A_0 e^{ikx} + B_0 e^{-ikx}\right)Z_0(z, h) + \sum_{n=1}^{\infty}\left(A_n e^{k_n x} + B_n e^{-k_n x}\right)Z_n(z, h), \tag{2.5}$$

for some constants A_n, B_n ($n \geq 0$). Here we have written

$$Z_0(z, h) = c_0 \cosh k(z + h) \tag{2.6}$$

$$Z_n(z, h) = c_n \cos k(z + h) \qquad (n \geq 1) \tag{2.7}$$

where k denotes the positive real root of the dispersion relation

$$\sigma = k \tanh kh \tag{2.8}$$

5

and k_n are the positive, real roots of

$$\sigma = -k_n \tan k_n h, \qquad (2.9)$$

arranged so that $k_n \leq k_{n+1}$ $(n \geq 1)$. The coefficients in (2.6) and (2.7) are defined by

$$
\begin{aligned}
c_0 = c_0(h) &= 2\sqrt{k(2kh + \sinh(2kh))^{-1}}, & (2.10) \\
c_n = c_n(h) &= 2\sqrt{k_n(2k_n h + \sinh(2k_n h))^{-1}}, & (n \geq 1), \quad (2.11)
\end{aligned}
$$

which ensure that the functions $Z_n(h, z)$ $(n \geq 0)$ form a complete orthonormal set on $-h \leq z \leq 0$. The notation makes use of (2.8) and (2.9) to define $k = k(h)$ and $k_n = k_n(h)$ $(n \geq 1)$ implicitly.
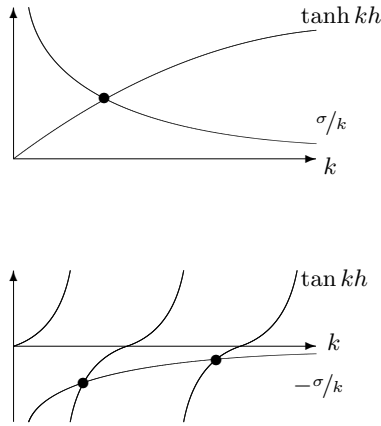
The two diagrams above correspond to equations (2.8) and (2.9) respectively. We can see that $\sigma = k \tanh kh$ has just the one positive solution. This represents a wave propagating through to infinity - a travelling wave. Whereas, $\sigma = -k_n \tan k_n h$ has infinitely many solutions, representing waves that decay exponentially.

The final conditions we require for the scattering problem are the conditions on the right and left - the radiation conditions. These follow from equation (2.5) and may be taken in the form

$$
\begin{aligned}
\phi(x, z) &\sim \left(A_- e^{ik_- x} + B_- e^{-ik_- x} \right) Z_0(z, h_-) & x \to -\infty, \quad (2.12) \\
\phi(x, z) &\sim \left(A_+ e^{-ik_+ x} + B_+ e^{ik_+ x} \right) Z_0(z, h_+) & x \to +\infty, \quad (2.13)
\end{aligned}
$$

6

where we have supposed that $h(x) \to h_\pm$ as $x \to \infty$ and written $k_\pm$ for the appropriate roots of the dispersion relation (2.8) corresponding to $h = h_\pm$. The

$$\begin{cases} e^{ikx} & \text{term represents right-travelling waves and} \\ e^{-ikx} & \text{term represents left-travelling waves,} \end{cases}$$

and $A_\pm$ and $B_\pm$ are the amplitudes of the corresponding waves, i.e. $A_\pm$ are the amplitudes of the incoming waves and $B_\pm$ are the amplitudes of the outgoing waves. This is illustrated below where we can see a cross-section of a water bed that has two constant, but different heights either side of a region of length ℓ, that has varying height.
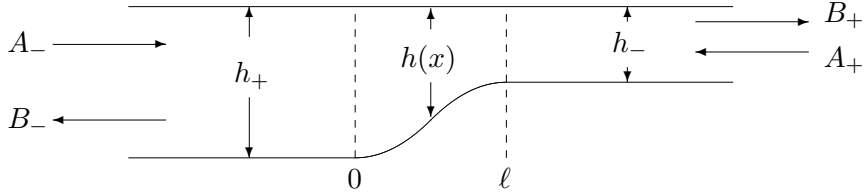
Let us focus on the two different areas of constant depth for a moment. Now if we recall equation (2.5) we can see that as $x \to -\infty$, we must have $B_n = 0$ ($n \geq 1$), thus preventing the solution from 'blowing up'. Furthermore, we can state that $A_0 = A_-$ and $B_0 = B_-$. Similarly, as $x \to +\infty$, $A_n = 0$ ($n \geq 1$), $B_0 = A_+$ and $A_0 = B_+$.

As the boundary value problem is linear, we can separate this general scattering problem into the two special cases below
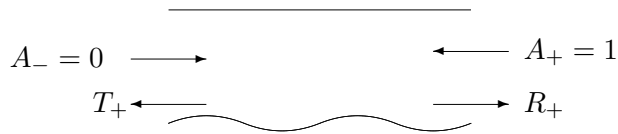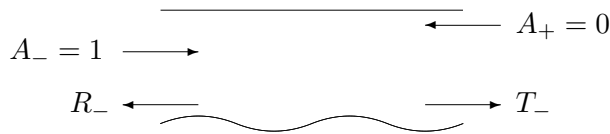
where $R_\pm$ are defined as the reflection coefficients and $T_\pm$ are defined as the transmission coefficients. From the diagrams we can see that the amplitudes of

the outgoing waves, $B_\pm$, are

$$A_- = 1, \quad A_+ = 0 : \qquad\qquad B_- = R_-, \quad B_+ = T_- \qquad\qquad (2.14)$$

$$A_- = 0, \quad A_+ = 1 : \qquad\qquad B_+ = R_+, \quad B_- = T_+ \qquad\qquad (2.15)$$

Due to linear theory, we can put these two separated cases back together to return to the general case. So the amplitudes of outgoing waves and amplitudes of incoming waves are therefore related by

$$\begin{pmatrix} B_- \\ B_+ \end{pmatrix} = \begin{pmatrix} R_- & T_+ \\ T_- & R_+ \end{pmatrix} \begin{pmatrix} A_- \\ A_+ \end{pmatrix} \equiv S \begin{pmatrix} A_- \\ A_+ \end{pmatrix}$$

where the scattering matrix S provides a complete description of the scattering process.

2.3   Derivation of the Modified Mild-Slope Equation

Continuing with a cross-section of the water bed, let us investigate what happens when h varies. We shall start by assuming

$$\phi(x, z) \approx \widehat{\phi}(x, z) = \phi_0(x) Z_0(z, h(x)). \qquad\qquad (2.16)$$

Ideally, we would have $\nabla^2 \widehat{\phi} = 0$, however, this is not the case - although it is close to zero. So to work around this, we take the weak form of $\nabla^2 \phi = 0$, in our aim to make $\nabla^2 \widehat{\phi}$ orthogonal to $Z_0(z, h(x))$. Thus we require

$$\int_{-h}^{0} \nabla^2 \widehat{\phi} Z_0\left(z, h(x)\right) dz = 0 \qquad\qquad (2.17)$$

so that

$$\int_{-h}^{0} \nabla^2 (\phi_0 Z_0) Z_0 \ dz = 0 \qquad\qquad (2.18)$$

i.e.

$$\int_{-h}^{0} \left((\phi_0 Z_0)_{xx} + (\phi_0 Z_0)_{yy} \right) Z_0 \ dz = 0 \qquad\qquad (2.19)$$

or equivalently

$$\int_{-h}^{0} (\phi_{0_{xx}}Z_0 + 2\phi_{0_x}Z_{0_x} + \phi_0 Z_{0_{xx}} + \phi_0 Z_{0_{yy}})Z_0 \ dz = 0. \tag{2.20}$$

Now, $Z_{0_{yy}} = k^2 Z_0$, and $\int_{-h}^{0} (\phi_0'' Z_0 + 2\phi_0' Z0_x)Z_0 \ dz = \left(\int_{-h}^{0} \phi_0' Z_0^2 \ dz\right)'$, so if we write $u_0 = \int_{-h}^{0} Z_0^2 \ dz$, equation (2.20) can be expressed as

$$(u_0\phi_0')' + k^2 u_0\phi_0 + v\phi_0 = 0, \tag{2.21}$$

where $v = \int_{-h}^{0} \phi_0 Z_0' Z_0 \ dz$ and the dash notation indicates differentiation with respect to x. It can further be shown that $v = u_1 h'' + u_2 h'^2$, for certain functions $u_1 = u_1(h)$, $u_2 = u_2(h)$ (see Chamberlain and Porter (1995) for details), so that we have

$$(u_0\phi_0')' + (k^2 u_0 + u_1 h'' + u_2 h'^2)\phi_0 = 0. \tag{2.22}$$

This process has averaged over the vertical axis to remove z components, so we are now dealing with just the one dimension (in x).

The last equation above (2.22) is the modified mild-slope equation. In the general three-dimension case it is

$$\nabla_h . u_0 \nabla_h \phi_0 + (u_0 k^2 + u_1 \nabla_h^2 h + u_2 (\nabla_h h)^2)\phi_0 = 0. \tag{2.23}$$

We have now seen how the modified mild-slope equation is technically derived, we shall later discuss why it was developed.

2.4 Derivation of the Mild-Slope Equation

So far, we have made the main assumption that the

- vertical structure of the velocity potential is equal, locally, to its behaviour over a flat bed.

A further assumption that has been widely used is that

- terms involving either the second derivatives or square of first derivatives of the still water depth function are negligible,
  i.e. $\nabla_h^2 h \approx (\nabla_h h)^2 \approx 0$.

Note that these assumptions are satisfied when h is constant. The second assumption allows us to simplify equation (2.23) to the mild-slope equation

$$\nabla_h.u_0\nabla_h\phi_0 + u_0k^2\phi_0 = 0. \tag{2.24}$$

The mild-slope equation was first presented by Berkhoff (1973, 1976).

2.5 Discussing the Modified Mild-Slope Equation and Mild-Slope Equation

It is worth mentioning at this point, that the validity of the second assumption ($\nabla_h^2 h \approx (\nabla_h h)^2 \approx 0$) has since been queried. Whilst it may seem that it is plausible as long as the depth varies 'slowly' in some sense - recent work has shown that the effect of $\nabla_h^2 h$ is more important than previously thought. Nonetheless, experiments carried out have led to the belief that the mild-slope equation is capable of providing excellent approximations which display the correct refraction, diffraction and scattering properties.

Other methods for solving these problems involve finding the diffraction solution for constant depth and then superimposing the reflection solution. These methods are questionable as it assumes reflection and diffraction are independent of each other.

It was observed by a number of authors that the mild-slope equation failed to produce adequate approximations for certain types of topography, such as ripple beds. These consist of a finite patch of small-amplitude sinusoidal ripples set in an otherwise horizontal bed. To overcome this deficiency in the mild-slope equation, numerous authors developed different methods to model ripple bed problems.

- Kirby (1986) presented a model in which the bed profile consists of a slowly varying (mild-slope) component on which is superimposed a rapidly varying component of small amplitude. Applying the vertical integration process led to what is now called the extended mild-slope equation.

- Massel (1993) proposed an approximation which combines the basic single-term mild-slope approximation with additional terms containing eigenfunctions corresponding to a number of evanescent modes. It is therefore capable of dealing with relatively steep bed profiles.

Chamberlain and Porter (1995) used the relatively simple type of approximation used by Berkhoff (1973, 1976) and Kirby (1986) to present the modified mild-

slope equation.

2.6 Multi-Mode Approximations

The reader should now be familiar with one method that is used to obtain the mild-slope equation and one of its variants - the modified mild slope equation. As we have seen, a clear benefit of using the mild-slope equation (or a variant of it), is its manner of reducing the dimension of the problem.

However, the drawback in using the mild-slope approximation is that its accuracy is not known. It was stated at the beginning of Section 2.4 that the results obtained are likely to be reasonably good approximations if the topography is slowly varying. But even in this case the derivation does not lead to an error term that can be estimated. To obtain more reliable quantative information further terms must be included in the approximation. Massel (1993) conducted this in the manner described in Section 2.5 by using Galerkin's method. Porter and Staziker (1995) also implemented the same concept by invoking a variational principle. It was shown that, by including N additional terms and increasing N until a desired accuracy has been reached, the removal of the vertical coordinate again simplifies the problem when the extended 'multi-mode' approximation is used but the modified mild-slope equation is replaced by $N+1$ coupled partial differential equations in the horizontal variables.

2.7 Acoustic Wave Transmission

We have seen how the mild-slope equation and the modified mild-slope equation can be used to approximate wave scattering over an uneven water bed. This project looks at how we can adapt these methods to approximate a different problem: acoustic wave transmission through ducts.

11
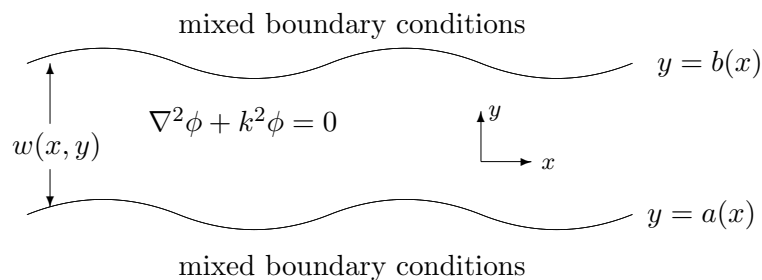
The diagram above illustrates our new, acoustic, problem. The differences between this problem and the previous water-bed problem are that

- we are working with the Helmholtz equation instead of Laplace's equation,

- we are no longer assuming the top boundary is linear, i.e., both the top and bottom boundaries may vary,

- we have different boundary conditions on the top and bottom of the duct, whereas previously the assumptions of water wave theory determined these boundary conditions.

The Helmholtz equation is used as linear acoustic waves are governed by the two-dimensional wave equation

$$\nabla^2 \widehat{\phi} - c^2 \widehat{\phi}_{tt} = 0, \tag{2.25}$$

where c is the sound speed. Now if we assume harmonic time-dependence, i.e., $\widehat{\phi}(x, y, t) = \phi(x, y)e^{-i\omega t}$, then the equation above becomes

$$\nabla^2 \phi + k^2 \phi = 0 \tag{2.26}$$

where $k = \omega/c$ is a wave number.

This dissertation will only be working with Dirichlet boundary conditions on both the top and bottom of the duct. We will be looking at single mode approximations for both a scattering and a trapped wave, as well as exploring the scattering problem further for multi-mode approximation.

Suppose we have a duct like below, where there are two different regions of constant height either side of a varying region.
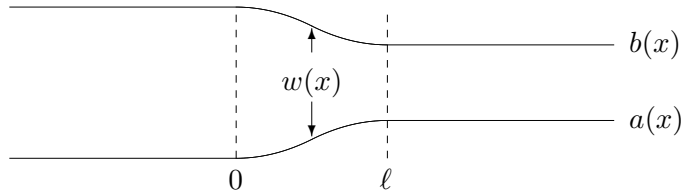
We require $a(x)$ and $b(x)$ to be uniform outside a finite region $0 < x < \ell$, and write

$$a(x) = \begin{cases} a_0 & x \leq 0 \\ a_1 & x \geq \ell \end{cases} \qquad b(x) = \begin{cases} b_0 & x \leq 0 \\ b_1 & x \geq \ell. \end{cases}$$

Within these uniform regions, a' and b' are zero.

Furthermore, we shall restrict attention to the case where the undulating

duct walls meet the uniform regions smoothly, i.e., we require that $a'(0) = b'(0) = a'(\ell) = b'(\ell) = 0$.

Chapter 3

Single Mode Approximations

3.1 A Scattering Problem

3.1.1 Regions Of Constant Width

To start, we shall examine the areas of constant width and separate the variables as previously done for the water wave problem. In uniform regions we write

$$\phi(x, y) = u(x)Y(y), \tag{3.1}$$

and separating the variables gives

$$\frac{u''}{u} + \frac{Y''}{Y} + k^2 = 0, \tag{3.2}$$

$$\Rightarrow \frac{u''}{u} + k^2 = -\frac{Y''}{Y} = \nu, \tag{3.3}$$

where ν is a separation constant.

In the y direction we have

$$Y'' + \nu Y = 0. \tag{3.4}$$

This has the general solution

$$
\begin{aligned}
Y(y) &= A\cos(\sqrt{\nu}y) + B\sin(\sqrt{\nu}y) \\
&= \widetilde{A}\sin\left[\sqrt{\nu}(y - a)\right],
\end{aligned} \tag{3.5}
$$

where the second form ensures that the Dirichlet condition at $y = a$ is satisfied, and $\widetilde{A}$ is a constant. Now, there are two different areas of constant width, so hence there are two different values of a (and b) for (3.5), and consequently

there are two different ν. We shall use the notation $\nu^{(j)}$ to correspond with a_j and b_j, where $j = 0, 1$.

To obtain $\nu^{(j)}$ we use the conditions determined by the Dirichlet boundary conditions, namely $Y(b_j) = 0$, hence

$$\widetilde{A} \sin \left[\sqrt{\nu^{(j)}}(b_j - a_j) \right] = 0, \qquad j = 0, 1. \tag{3.6}$$

For this to be the case, we must have

$$
\begin{aligned}
\sqrt{\nu_n^{(j)}}(b_j - a_j) &= n\pi, \\
\Rightarrow \nu_n^{(j)} &= \frac{n^2 \pi^2}{(b_j - a_j)^2}. \qquad j = 0, 1 \text{ and } n = 1, 2, ... \tag{3.7}
\end{aligned}
$$

Finally, choosing $\widetilde{A} = 1$ we have

$$Y_n(y) = \sin \left(\frac{n\pi(y - a_j)}{b_j - a_j} \right). \qquad j = 0, 1 \text{ and } n = 1, 2, ... \tag{3.8}$$

Let us return to equation (3.3), this time taking the equation in the x direction,

$$u_n'' + (k^2 - \nu_n)u_n = 0. \qquad n = 1, 2, ... \tag{3.9}$$

This has solution

$$u_n(x) = A_n e^{i\kappa_n^{(j)} x} + B_n e^{-i\kappa_n^{(j)} x}, \qquad j = 0, 1 \text{ and } n = 1, 2, ... \tag{3.10}$$

where $\kappa_n^{(j)2} = k^2 - \nu_n^{(j)}$. Note that if $\kappa_n^{(j)}$ is real, i.e. if $n < \frac{k(b_j - a)j)}{\pi}$, then equation (3.10) represents propagating modes. Otherwise, if $\kappa_n^{(j)}$ is imaginary, then $\pm i\kappa_n^{(j)}$ is real, and the modes are evanescent. We restrict our attention to the case for which a single mode propagates, i.e we require the wall profiles $a(x)$ and $b(x)$ to satisfy

$$1 < \frac{k}{\pi}(b - a) < 2. \tag{3.11}$$

Hence the most general solution is

$$\phi = \sum_{n=1}^{\infty} u_n(x) Y_n(y). \tag{3.12}$$

For now, we shall make the approximation to proceed with only the single mode, $n = 1$. By doing this we are assuming that the vertical structure of the

velocity potential is equal, locally, to its behaviour over a flat bed - this is a key assumption of the mild-slope equation which was discussed earlier in this dissertation.

3.1.2 Undulating Regions

Taking the earlier assumption into consideration, let us move onto the undulating regions where u_1 depends on both x and y. Let

$$\phi(x, y) \approx u_1(x, y)Y_1(y, a, b), \tag{3.13}$$

where $a = a(x)$, $b = b(x)$ and $Y_1 = \sin\left(\frac{\pi(y-a)}{b-a}\right)$.

When working with the water wave problem, the weak form of Laplace's equation was taken. So for this new problem we shall take the weak form of the Helmholtz equation to force the result

$$\int_a^b (\nabla^2(u_1Y_1) + k^2 u_1 Y_1)Y_1 dy = 0, \tag{3.14}$$

where $u_1Y_1 = u_1(x)Y_1(y, a, b)$ and a, b, and Y_1 are defined as earlier.

Next, we rearrange equation (3.14) to give us as an ordinary differential equation (ODE) in terms of u_1 and its x derivatives. Let us begin with the term

$$\nabla^2(u_1Y_1) = (u_1Y_1)_{xx} + (u_1Y_1)_{yy}. \tag{3.15}$$

When we break this down we get

$$
\begin{aligned}
(u_1Y_1)_x &= u_{1_x}Y_1 + u_1Y_{1_x}, &\tag{3.16}\\
(u_1Y_1)_{xx} &= u_{1_{xx}}Y_1 + 2u_{1_x}Y_{1_x} + u_1Y_{1_{xx}}, &\tag{3.17}\\
(u_1Y_1)_y &= u_1Y_{1_y}, &\tag{3.18}\\
(u_1Y_1)_{yy} &= u_1Y_{1_{yy}}. &\tag{3.19}
\end{aligned}
$$

Substituting these values back into (3.14) gives

$$
\begin{aligned}
0 &= \int_a^b \left[(u_1 Y_1)_{xx} + (u_1 Y_1)_{yy} + k^2 u_1 Y_1 \right] Y_1 \ dy \\
&= \int_a^b \left[u_{1_{xx}} Y_1 + 2 Y_{1_x} u_{1_x} + u_1 (Y_{1_{xx}} + Y_{1_{yy}} + k^2 Y_1) \right] Y_1 \ dy \\
&= \alpha u_1'' + \alpha' u_1' + (\beta + \gamma + k^2 \alpha) u_1 \\
&= (\alpha u_1')' + (\beta + \gamma + k^2 \alpha) u_1
\end{aligned}
\tag{3.20}
$$

where $(.)'$ denotes the differentiation with respect to x,

$$
\alpha = (Y_1, Y_1), \qquad \beta = (Y_1'', Y_1), \qquad \gamma = (Y_{1_{yy}}, Y_1), \tag{3.21}
$$

and the brackets denote the inner product notation

$$
(f, g) = \int_a^b f(y) \overline{g}(y) \ dy. \tag{3.22}
$$

Now we are required to compute the coefficients we have just defined.

$$
\begin{aligned}
\alpha &= (Y_1, Y_1), & (3.23) \\
&= \int_a^b \sin^2 \left(\frac{\pi(y - a)}{b - a} \right) \ dy, & (3.24) \\
&= \frac{1}{2}(b - a). & (3.25)
\end{aligned}
$$

$$
\begin{aligned}
\beta &= (Y_1'', Y_1), & (3.26) \\
&= \int_a^b \left[\left(a' Y_{1_{aa}} + b' Y_{1_{ab}} \right) a' + \left(a' Y_{1_{ab}} + b' Y_{1_{bb}} \right) b' \right. \\
&\qquad \left. + a'' Y_{1_a} + b'' Y_{1_b} \right] Y_1 \ dy, & (3.27) \\
&= \frac{1}{12(b - a)} \left\{ 3 b''(b - a) - 3 a''(b - a) - 3(b' - a')^2 \right. \\
&\qquad \left. - 2\pi^2 (a'^2 + b'^2 + a' b') \right\}. & (3.28)
\end{aligned}
$$

$$
\begin{aligned}
\gamma &= (Y_{yy}, Y), & (3.29) \\
&= \int_a^b Y_1 Y_{1_{yy}} \ dy, & (3.30) \\
&= \frac{\pi^2}{2(a - b)}, & (3.31) \\
&= -\frac{\pi^2 \alpha}{(b - a)^2}. & (3.32)
\end{aligned}
$$

Note that $\beta = 0$ when $a' = b' = a'' = b'' = 0$.

Finally, we have all the components of the ODE. Later, we will determine the boundary conditions for the undulating region, thus enabling us apply an ODE solver to (3.20) so that we may acquire $u_1(x)$ in the region $0 < x < \ell$.

Suppose we have a scattering problem as below:
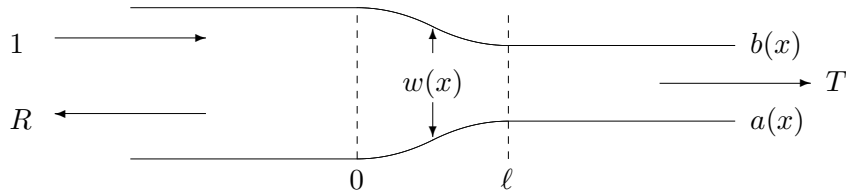
Earlier, we defined u_1 in the constant regions as equation (3.9). Using this we can write

$$u_1(x) = e^{i\kappa_1^{(0)}x} + Re^{-i\kappa_1^{(0)}x}, \tag{3.33}$$

for $x < 0$, since there is an incident right travelling wave with an amplitude of one, along with a reflected wave of amplitude R..

Similarly, for $x > \ell$ we write

$$u_1(x) = Te^{i\kappa_1^{(1)}x}, \tag{3.34}$$

to ensure there is an outgoing wave only, the transmitted wave.

3.1.3   Determining The Boundary Conditions

The previous subsection provided us with information for $u_1(x)$ over the whole region. The next step is to determine the boundary conditions on either side of the undulating region. This needs to be approached in a manner that eliminates R and T as they are unknown at this point. For continuity, the value of u_1 just to the left of $x = 0$ will equal the value of u_1 just to the right of $x = 0$, as will the derivatives of u_1. Consequently we must have

$$
\begin{aligned}
u_1(0^-) &= u_1(0^+) & (3.35) \\
u_1'(0^-) &= u_1'(0^+) & (3.36)
\end{aligned}
$$

where $u_1(0^\pm)$ denotes u_1 slightly to the left or right of zero accordingly, and similarly for $u_1(\ell)$. So we require (3.33) to match (3.13) at $x = 0$, and similarly

for their derivatives. This produces

$$
\begin{aligned}
u_1(0^-) &= 1 + R, & (3.37) \\
u_1'(0^-) &= i\kappa_1^{(0)}(1 - R), & (3.38) \\
\Rightarrow u_1'(0^+) + i\kappa_1^{(0)}u_1(0^+) &= i\kappa_1^{(0)}(1 - R) + i\kappa_1^{(0)}(1 + R) \\
\Rightarrow 0 &= u_1'(0) + i\kappa_1^{(0)}u_1(0) - 2i\kappa_1^{(0)}. & (3.39)
\end{aligned}
$$

The right-hand boundary condition is found using similar reasoning with (3.34) matching (3.13) at $x = \ell$ to give

$$
0 = u_1'(\ell) - i\kappa_1^{(1)}u_1(\ell). \tag{3.40}
$$

3.1.4 Calculating the Velocity Potential ϕ Over The Whole Duct

To calculate ϕ in the undulating region, we must first solve equation (3.20) with (3.39) and (3.40) as the boundary conditions. This is done using a Matlab built-in programme, `bvp4c`, which solves boundary value problems for ODEs. This is an effective solver, but the underlying method and the computing environment are not appropriate for high accuracies nor for problems with extremely sharp changes in their solutions.

When using `bvp4c`, the user is required to create two function handles. One function handle evaluates the differential equation (3.20) as a system of first order ODEs. To do this, we let $v_1 = \alpha u_1'$, thus providing us with a suitable system,

$$
\begin{pmatrix} u_1 \\ v_1 \end{pmatrix}' = \begin{pmatrix} 0 & \alpha^{-1} \\ -(\beta + \gamma + k^2\alpha) & 0 \end{pmatrix} \begin{pmatrix} u_1 \\ v_1 \end{pmatrix}.
$$

The other function handle computes the residual in the boundary conditions, so it is simply a case of applying the equations (3.39) and (3.40).

Equations (3.33) and (3.34) provided us with values for $u_1(x)$ in the regions of constant width, and involve the unknowns R and T. Due to continuity, and provided the three different regions of $a(x)$ and $b(x)$ join smoothly, we can calculate R and T using the values of $u(0)$ and $u(\ell)$ obtained from solving the ODE (3.20). Starting with $x = 0$, we derive R by

$$
\begin{aligned}
u_1(0) &= 1 + R, \\
\Rightarrow R &= u_1(0) - 1. \tag{3.41}
\end{aligned}
$$

And similarly, for $x = \ell$, T is defined as

$$u_1(\ell) = Te^{i\kappa_1^{(1)}\ell},$$
$$\Rightarrow T = \frac{u_1(\ell)}{e^{i\kappa_1^{(1)}\ell}}. \tag{3.42}$$

One can easily check their values of R and T by checking that the following holds,

$$|R|^2 + |T|^2 = 1. \tag{3.43}$$

This result is due to energy conservation being implemented on the incoming wave with amplitude one. Once our ODE is solved, we possess the values of R and T. By substituting the newly established coefficients back into (3.33) and (3.34), we can explicitly compute $u_1(x)$ over the whole duct. This means we can approximate ϕ over the whole duct by using (3.13). The numerical results are given later in Chapter 5.

3.2 A Trapped Wave Problem

3.2.1 Deriving An Expression For $u_1(x)$

Another situation to analyse is the wave trapping problem. For this problem there would not be any reflection nor transmission as we are dealing with waves that decay exponentially outside the varying segment of the duct. For $0 < x < \ell$, $u_1(x)$ will still be defined by the ODE (3.20). However, we need to obtain new expressions for $u_1(x)$ to the left and right of the undulating region.

To do this, let us return to equation (3.9). From this, we write that in regions of constant width, $u_1(x)$ is defined as

$$u_1(x) = Ae^{\sqrt{\nu_1 - k^2}x} + Be^{-\sqrt{\nu_1 - k^2}x}. \tag{3.44}$$

Since we require exponentially decaying solutions in the x direction we require $\nu_1 > k^2$.

We must also consider the radiation conditions, $\phi \to 0$ as $|x| \to \infty$. Therefore, for $x < 0$ we require $B = 0$, and for $x > \ell$ we require $A = 0$

$$u_1(x) = \begin{cases} Ae^{\sqrt{\nu_1^{(0)} - k^2}x} & x < 0 \\ Be^{-\sqrt{\nu_1^{(1)} - k^2}x} & x > \ell. \end{cases} \tag{3.45}$$

3.2.2   Determining The Boundary Conditions

As with the travelling wave problem, to determine the boundary conditions at $x = 0$ and $x = \ell$ we assume that the regions of the duct are joined smoothly at these two points. Then we require that the pressure and its gradient are continuous at $x = 0$, from which we must have

$$u_1(0^-) = u_1(0^+), \tag{3.46}$$

$$u_1'(0^-) = u_1'(0^+), \tag{3.47}$$

where $u_1(0^\pm)$ denotes u_1 slightly to the left or right of zero accordingly, and similarly for $u_1(\ell^\pm)$.

We use (3.45) from the previous subsection to determine $u_1(0^-)$ and $u_1'(0^-)$ and then combine them in a manner that eliminates the unknown A.

$$u_1(0^-) = A, \tag{3.48}$$

$$u_1'(0^-) = A\sqrt{\nu_1^{(0)} - k^2}, \tag{3.49}$$

$$\Rightarrow u_1'(0^+) - \sqrt{\nu_1^{(0)} - k^2}u_1(0^+) = A\sqrt{\nu_1^{(0)} - k^2} - \sqrt{\nu_1^{(0)} - k^2}A$$

$$\Rightarrow u_1'(0) - \sqrt{\nu_1^{(0)} - k^2}u_1(0) = 0. \tag{3.50}$$

Using the same approach for $x = \ell$ gives

$$u_1'(\ell) + \sqrt{\nu_1^{(1)} - k^2}u_1(\ell) = 0 \tag{3.51}$$

3.2.3   Solving The Eigenvalue Problem

Firstly, it should be mentioned that this is an eigenvalue problem. There may not necessarily be any eigenvalues, indicating that there is not a trapped wave. So to start, we must find the values of k for which there is a trapped wave.

One method of approach is to use an initial value problem (IVP) solver to solve (3.20) along with (3.50) split into two initial conditions like so

$$u_1(0) = 1, \tag{3.52}$$

$$u_1'(0) = \sqrt{\nu_1^{(0)} - k^2}, \tag{3.53}$$

for $0 < k < \sqrt{\nu_1^{(0)}}$.

Next, we plot the left-hand side of the second boundary condition (3.51) against k using the solutions from the IVP solver to derive $u_1'(\ell)$ and $u_1(\ell)$. The

roots of this function, if any, are the eigenvalues.

The roots of the plot can be found using the bisection method, which is a root-finding algorithm that works by repeatedly dividing an interval in half and then selecting the subinterval in which the root exists. The absolute error for the bisection method is halved at every step, so the method converges linearly. Although the bisection method is slower to converge than other methods such as the regular Falsi method, it is suitable for what we require here, and is guaranteed to converge if the function crosses the x-axis.

Matlab's built-in IVP solver, `ode23` is suitable to solve (3.20). The function `ode23` is an implementation of second/third-order Runge-Kutta methods. To use `ode23` we are required to create a function handle that, given the scalar x and vector $\mathbf{z}$ as input, returns the x derivative vector $\mathbf{z}$' as output. This requires our ODE (3.20) to be recast as a system of first order equations. Let us introduce two new variables, $z_1 = u_1$ and $z_2 = u_1'$. Then $z_1' = u_1' = z_2$ and $z_2' = u_1'' = \frac{-\alpha' z_2 + (\beta + \gamma + k^2 \alpha) z_1}{\alpha}$. Now equation (4.19) can be written in vector form as

$$
\begin{pmatrix} z_1 \\ z_2 \end{pmatrix}' = \begin{pmatrix} z_2 \\ \alpha^{-1}(-\alpha' z_2 + (\beta + \gamma + k^2 \alpha) z_1) \end{pmatrix}.
$$

The right-hand side of this system is used in the function handle, so that when `ode23` is run, the output $\mathbf{z}$ contains two columns: z_1 which is actually $u_1(x)$, and z_2, which is $u_1'(x)$.

Once we have computed $u_1(x)$ over the varying region, we can use the values of $u_1(0)$ and $u_1(\ell)$ to derive A and B in equations (3.45) - thus enabling us to obtain $u_1(x)$ for $x < 0$ and $x > \ell$. And as we know Y_1 over the whole duct, we can now approximate ϕ over the whole duct using (3.13). The numerical results are given later in Chapter 5.

Chapter 4

Including More Modes

4.1 Deriving A System Of Ordinary Differential Equations

In Section 3.1.1 we found the general solution, in uniform regions, to be

$$\phi = \sum_{n=1}^{\infty} u_n(x) Y_n(y).$$

where

$$Y_n(y) = \sin\left(\frac{n\pi(y - a_j)}{b_j - a_j}\right) \qquad j = 0, 1.$$

In Chapter 3 we worked with a single mode, meaning we were only working with $n = 1$. Now suppose we look at N modes, implying that for regions of uniform width of the duct,

$$\phi \approx \sum_{n=1}^{N} u_n(x) Y_n(y). \tag{4.1}$$

In a similar fashion to the single-mode case, we now use the representation (4.1) to motivate an appropriate form of ϕ in regions where the duct side-walls undulate. Thus we write

$$\phi \approx \widetilde{\phi} = \sum_{n=1}^{N} u_n(x) Y_n(x, y) \tag{4.2}$$

where now

$$Y_n(x, y) = \sin\left(\frac{n\pi(y - a)}{b - a}\right) \qquad n = 1, 2, ...N. \tag{4.3}$$

Since we cannot expect $(\nabla^2 + k^2)\widetilde{\phi} = 0$, we require a weak form of the Helmholtz equation written as

$$\int_a^b (\nabla^2 + k^2)\, \widetilde{\phi}\, Y_m\ dy = 0 \qquad m = 1, 2, ...N. \tag{4.4}$$

Let us begin by examining $(\nabla^2 + k^2)\widetilde{\phi}$. We find that

$$
\begin{aligned}
(\nabla^2 + k^2)\widetilde{\phi} &= (\nabla^2 + k^2)\sum_{n=1}^{N} u_n Y_n \\
&= \sum_{n=1}^{N} \left\{(u_n Y_n)_{xx} + (u_n Y_n)_{yy} + k^2 u_n Y_n\right\} \\
&= \sum_{n=1}^{N} \left\{u_n'' Y_n + 2u_n' Y_{n_x} + u_n Y_{n_{xx}} + u_n Y_{n_{yy}} + k^2 u_n Y_n\right\} \\
&= \sum_{n=1}^{N} \left\{u_n'' Y_n + 2u_n' Y_{n_x} + (Y_{n_{xx}} + Y_{n_{yy}} + k^2 Y_n)u_n\right\} \tag{4.5}
\end{aligned}
$$

Substituting (4.5) back into (4.4) show that for any N there will be a system of N equations in the N unknowns $u_1, ..., u_N$. When making this substitution, the coefficients of u_n can be presented in a similar fashion to the single mode approximation:

$$\sum_{n=1}^{N} \left(\alpha_{m,n} u_n'\right)' + \left(\beta_{m,n} + \gamma_{m,n} + k^2 \alpha_{m,n}\right) u_n = 0, \qquad m = 1, 2, ...N, \tag{4.6}$$

where

$$\alpha_{m,n} = (Y_n, Y_m), \qquad \beta_{m,n} = (Y_n'', Y_m), \qquad \gamma_{m,n} = (Y_{n_{yy}}, Y_m) \tag{4.7}$$

and the brackets denote the inner product notation (3.22). For notation and programming reasons, we shall reformat equation (4.6) as

$$(\alpha \mathbf{u}')' + (\beta + \gamma + k^2 \alpha)\mathbf{u} = \mathbf{0} \tag{4.8}$$

where

$$\alpha = \begin{pmatrix} \alpha_{1,1} & \alpha_{1,2} & \cdots \\ \alpha_{2,1} & \ddots & \vdots \\ \vdots & \cdots & \alpha_{N,N} \end{pmatrix},$$

and similarly for β and γ. The vector $\mathbf{u}$ is defined as

$$\mathbf{u} = \begin{pmatrix} u_1 \\ u_2 \\ \vdots \\ u_N \end{pmatrix}.$$

So now we need to derive expressions for $\alpha_{m,n}$, $\beta_{m,n}$ and $\gamma_{m,n}$. We find that

$$\alpha_{m,n} = (Y_n, Y_m) \tag{4.9}$$

$$= \int_a^b \sin\left(\frac{n\pi(y-a)}{(b-a)}\right) \sin\left(\frac{m\pi(y-a)}{(b-a)}\right) \, dy \tag{4.10}$$

$$= \begin{cases} \frac{1}{2}(b-a) & m = n \\ 0 & m \neq n \end{cases} \tag{4.11}$$

$$\beta_{m,n} = (Y_n'', Y_m) \tag{4.12}$$

$$= \int_a^b \sin\left(\frac{m\pi(y-a)}{(b-a)}\right) \left[\left(a'Y_{n_{aa}} + b'Y_{n_{ab}}\right) a' + \left(a'Y_{n_{ab}} + b'Y_{n_{bb}}\right) b' \right. $$
$$\left. + a''Y_{n_a} + b''Y_{n_b} \right] \, dy \tag{4.13}$$

$$= \begin{cases} \frac{1}{12(b-a)}\{3b''(b-a) - 3a''(b-a) - 3(b'-a')^2 \\ \qquad -2n^2\pi^2((b')^2 + (a')^2 + a'b')\} & m = n \\[2mm] \frac{n}{(m^6 - n^6 - 3m^4 n^2 + 3m^2 n^4)(b-a)}\{a''(b-a)(2n^2 m^3 - n^4 m - m^5) \\ \qquad -2a'(b'-a')m(n^4 - m^4) + (-1)^{n+m}\left[b''(b-a)(m^5\right. \\ \qquad \left. -2n^2 m^3 + n^4 m) + 2(b')^2 m(n^4 - m^4) - 2a'b'm(n^4 \right. \\ \qquad \left. -m^4)\right] \} & m \neq n \end{cases} \tag{4.14}$$

$$\gamma_{m,n} = (Y_{n_{yy}}, Y_m) \tag{4.15}$$

$$= \int_a^b -\left(\frac{n\pi}{(b-a)}\right)^2 \sin\left(\frac{n\pi(y-a)}{(b-a)}\right) \sin\left(\frac{m\pi(y-a)}{(b-a)}\right) \, dy \tag{4.16}$$

$$= \begin{cases} -\frac{n^2\pi^2}{2(b-a)} & m = n \\ 0 & m \neq n \end{cases} \tag{4.17}$$

25

Note here that $\alpha_{m,n}$ does not depend on n nor m. So for any fixed value of x, α will be a constant multiple of the $N \times N$ identity matrix.

4.2   Defining A Scattering Problem

As with the single mode, we shall model the scenario below.
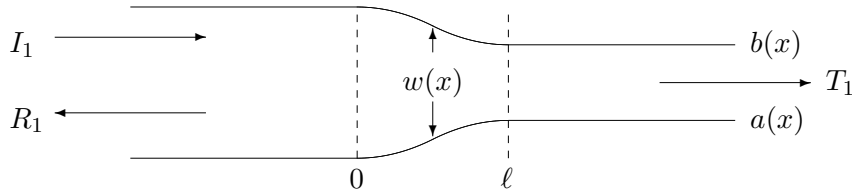
We shall restrict our attention to the case for which there is only a single propagating mode within the uniform sections of the duct, i.e. we require $1 < \frac{k}{\pi}(b - a) < 2$.

In $x < 0$, we write

$$\phi \approx \sum_{n=1}^{N} \left\{ I_n e^{i\kappa_n^{(0)} x} + R_n e^{-i\kappa_n^{(0)} x} \right\} Y_n(y), \tag{4.18}$$

where $I_1 = 1$ is the amplitude of the incident propagating mode, and we set $I_2 = \cdots = I_N = 0$ to ensure there are no exponentially growing waves in this region. Also, R_n is the (unknown) amplitude of the nth reflected mode.

In $0 < x < \ell$, we have the approximation

$$\phi \approx \sum_{n=1}^{N} u_n(x) Y_n(x, y). \tag{4.19}$$

These representations of the solution must be equal at the interface $x = 0$, as must their x derivatives. Thus, provided the regions either side of $x = 0$ join smoothly, we have

$$\sum_{n=1}^{N} (I_n + R_n) Y_n(y) = \sum_{n=1}^{N} u_n(0) Y_n(0, y) \tag{4.20}$$

$$\Rightarrow I_n + R_n = u_n(0), \qquad n = 1, 2, .., N, \tag{4.21}$$

and

$$\sum_{n=1}^{N} i\kappa_n^{(0)}(I_n - R_n)Y_n(y) = \sum_{n=1}^{N} u_n'(0)Y_n(0,y) \tag{4.22}$$

$$\Rightarrow i\kappa_n^{(0)}(I_n - R_n) = u_n'(0), \qquad n = 1, 2, .., N. \tag{4.23}$$

Upon eliminating the unknown R_n from these two equations, our first boundary condition is

$$u_n'(0) + i\kappa_n^{(0)}u_n(0) = 2i\kappa_n^{(0)}I_n \qquad n = 1, 2, .., N. \tag{4.24}$$

Following a similar procedure we can find the right-hand boundary condition. In $x > \ell$, we write

$$\phi \approx \sum_{n=1}^{N} T_n e^{i\kappa_n^{(1)}x}Y_n(y). \tag{4.25}$$

where T_n is the (unknown) coefficient of the nth transmitted mode. In $0 < x < \ell$, as before,

$$\phi \approx \sum_{n=1}^{N} u_n(x)Y_n(x,y). \tag{4.26}$$

As with the previous case, for continuity these two equations, and their derivatives, must be equal at the interface $x = \ell$. Thus

$$\sum_{n=1}^{N} T_n e^{i\kappa_n^{(1)}\ell}Y_n(y) = \sum_{n=1}^{N} u_n(\ell)Y_n(\ell,y) \tag{4.27}$$

$$\Rightarrow T_n e^{i\kappa_n^{(1)}\ell} = u_n(\ell) \tag{4.28}$$

and

$$\sum_{n=1}^{N} i\kappa_n^{(1)}T_n e^{i\kappa_n^{(1)}\ell}Y_n(y) = \sum_{n=1}^{N} u_n'(\ell)Y_n(\ell,y) \tag{4.29}$$

$$\Rightarrow i\kappa_n^{(1)}T_n e^{i\kappa_n^{(1)}\ell} = u_n'(\ell) \qquad n = 1, 2, .., N \tag{4.30}$$

Eliminating T_n, the unknown, from equations (4.28) and (4.30) brings us to our second boundary condition,

$$u_n'(\ell) - i\kappa_n^{(1)}u_n(\ell) = 0 \qquad n = 1, 2, .., N. \tag{4.31}$$

27

4.3 Calculating The Velocity Potential ϕ Over The Whole Duct

Solving the system of N equations with $2N$ boundary conditions is handled in a similar fashion to the single mode approximation in Section 3.1.4. Again, we take advantage of the Matlab programme `bvp4c` so we are required to adapt our system of second order ODEs into two systems of first order ODEs. Moreover, with the new scattering model we have matrices and vectors as components of the ODE system and boundary conditions. One method of approach is to create separate function handles to calculate the entries of the coefficient matrices: α, $\alpha_{\mathbf{x}}$, β, and γ. A further function handle is required to store these entries in appropriately named matrices. By making these separate function handles it keeps the main programme uncrowded so that it is easy to follow, and results in only defining each matrix once.

Chapter 5

Numerical Results

5.1 Scattering Problem

All the scattering problems discussed here satisfy the inequality (3.11) for all $a(x)$ and $b(x)$, thus ensuring the presence of one and only one propagating wave.

5.1.1 Single Mode Approximations

Two different categories of duct were modelled. The first, which will be referred to as duct (1), can be described by

$$a(x) = \begin{cases} 0 & x < 0 \\ d\sin^2\left(\frac{\pi x}{2\ell}\right) & 0 < x < \ell \\ d & x > \ell, \end{cases} \qquad (5.1)$$

and

$$b(x) = \begin{cases} 1 & x < 0 \\ 1 - a(x) & 0 < x < \ell \\ 1 - d & x > \ell. \end{cases} \qquad (5.2)$$

Figures (5.1), (5.2) and (5.1.1) refer to when $d = 0.1$, $k = 6$ and $\ell = 1$. We can see that there is more activity to the left of the duct than to the right. This shows that we have a large amount of reflection and not much transmission.

Figure (5.3) is an interesting plot. It shows the effect of increasing ℓ, so the slope of the duct walls for $0 < x < \ell$ is more gradual. The reflection oscillates greatly as ℓ is increased. Whilst the peaks remain at a constant at a little above $|R| = 0.9$, the troughs (where there is not much reflection) smoothly

29

vary. The first trough corresponds to $|R|$ approximately being 0.05. From here, as $k\ell$ increases each trough corresponds to more reflection than the previous until $k\ell$ is around 40 to 44. At this point, the troughs decrease to mirror the results on the left-hand side of this point. From this figure we conclude that the relection produced from duct (1) varies greatly depending on $k\ell$.

Now let us consider a duct that varies more smoothly, duct(2). The duct walls are defined as

$$a(x) = \begin{cases} 0 & x < 0 \\ d\sin^2\left(\frac{\mu\pi x}{\ell}\right) & 0 < x < \ell \\ 0 & x > \ell, \end{cases} \qquad (5.3)$$

and

$$b(x) = \begin{cases} 1 & x < 0 \\ 1 - a(x) & 0 < x < \ell \\ 1 & x > \ell. \end{cases} \qquad (5.4)$$

Figures (5.4), (5.5) and (5.6) refer to when $d = 0.1$, $\ell = 2$, $k = 4$ and $\mu = 1$. When comparing these results with the previous duct, we can see that there is much less reflection. Therefore, we can state that a duct of this shape allows more acoustic wave transmission than the previous duct shape. However, when μ is increased to eight so the duct walls have eight 'humps' for $0 < x < \ell$, we have a different conclusion. Figures (5.7), (5.8) and (5.9) show us that nearly all the energy has been reflected back.

The concept of there being more reflection when there are more 'humps' is explored further in figure (5.10). Each time μ increases, so does $k|R|$, especially for smaller ℓ. As the length of the undulating region increases there is less difference between the different μ. Indeed, for $\ell = 1$, the difference in $k|R|$ for $\mu = 1$ and $\mu = 2$ is minimal. For each μ, $k|R|$ seems to level off to a constant, and for larger μ this plateau is reached for smaller ℓ.

Figures (5.11) and (5.12) display $k|R|$ for varying d and ℓ. Figure (5.11) refers to when $\mu = 1$ and figure (5.12) refers to when $\mu = 2$. In both cases we can see that as ℓ and d increase, so does $k|R|$. Perhaps a surprising outcome is that varying ℓ has a more forceful effect on $k|R|$ than d, where d determines the size of the 'humps'. This is especially noticeable in (5.12) where the changes in $k|R|$ occur for smaller ℓ. The outcome that d created is similar for both μ.
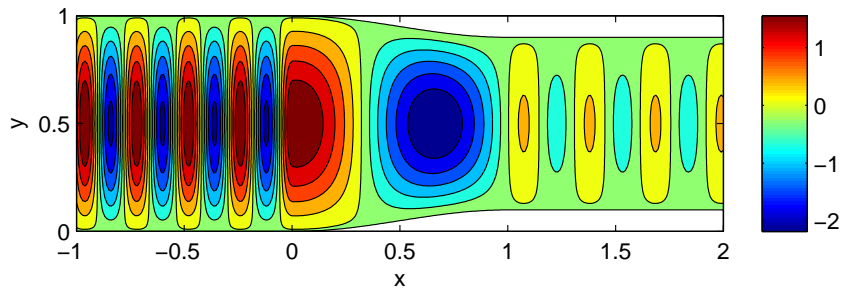
Figure 5.1: Contour plot of ϕ over duct (1).
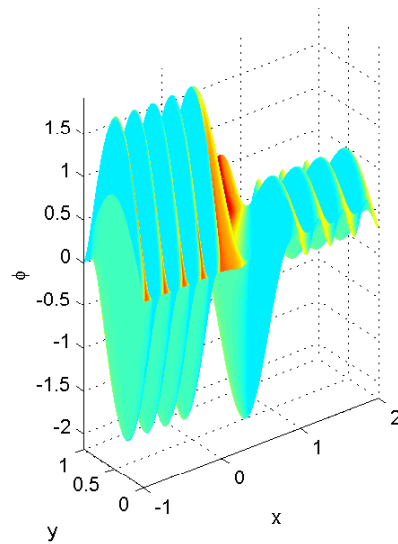
Figure 5.2: Surf plot of ϕ over duct (1).

31
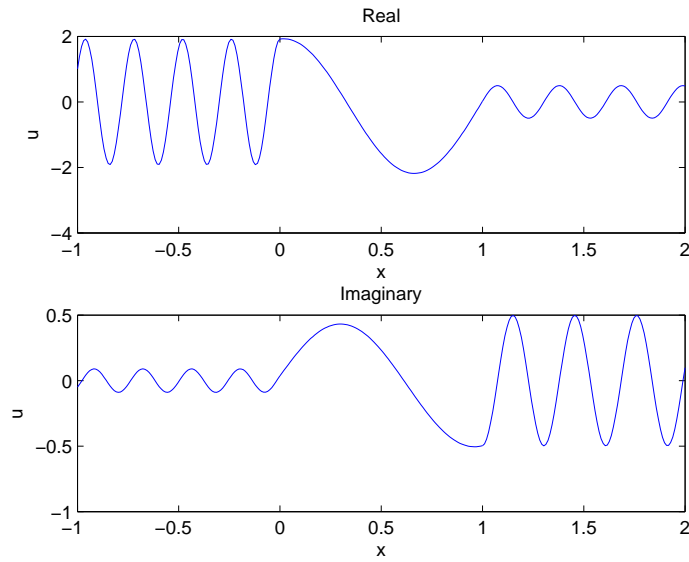
Figure 5.3: Real and imaginary plots of u over duct (1).
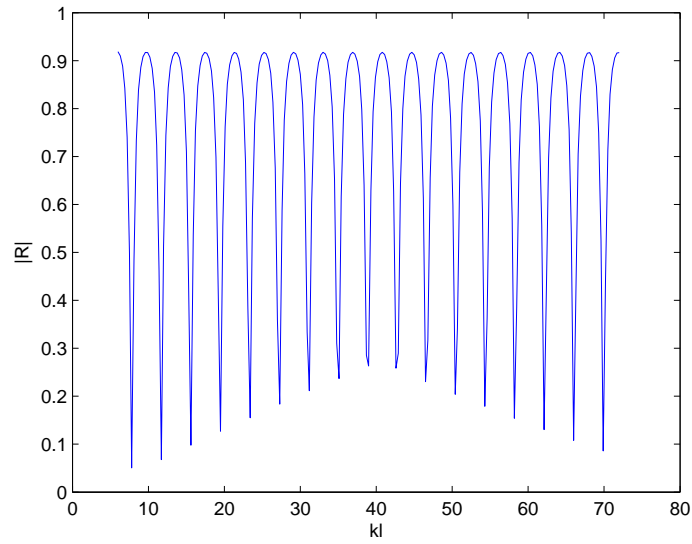
Figure 5.4: $|R|$ against $k\ell$ using duct(1), with fixed $k = 6$.
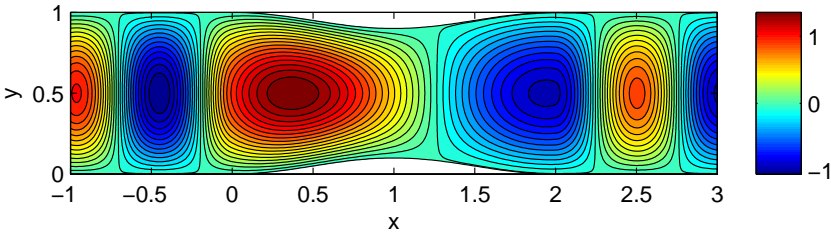
Figure 5.5: Contour plot of ϕ over duct (2).
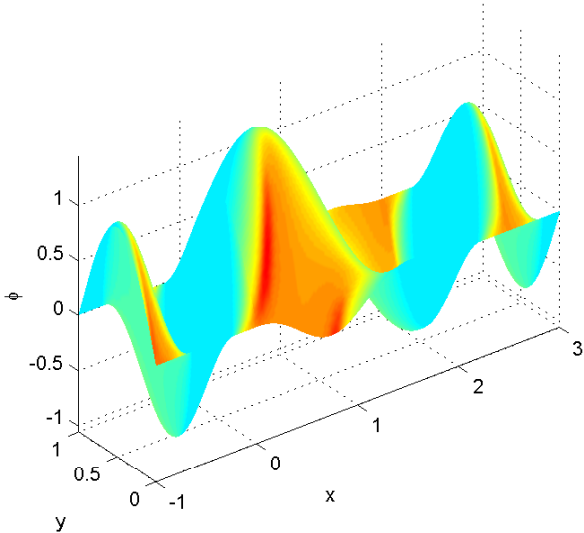
Figure 5.6: Surf plot of ϕ over duct (2).
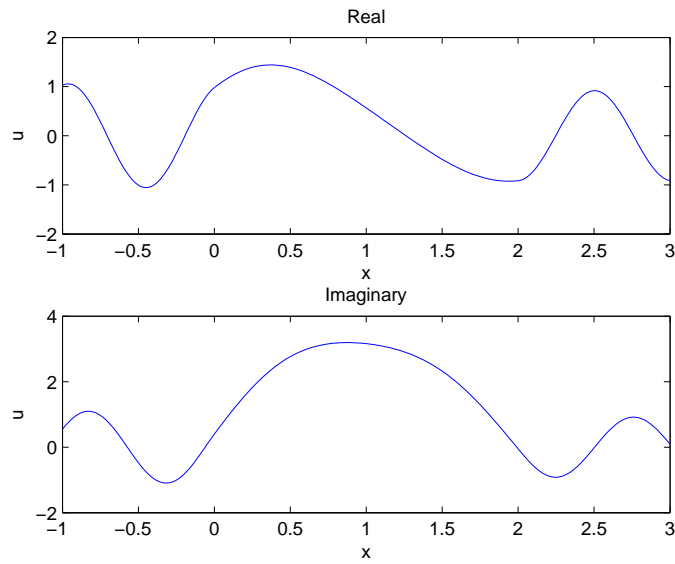
Figure 5.7: Real and imaginary plots of u over duct (2).
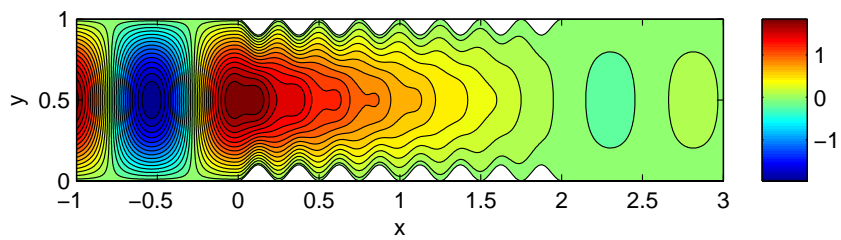
Figure 5.8: Contour plot of ϕ over duct (2).
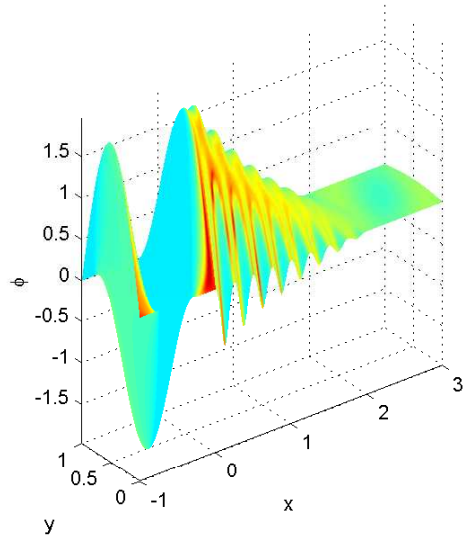
Figure 5.9: Surf plot of ϕ over duct (2).
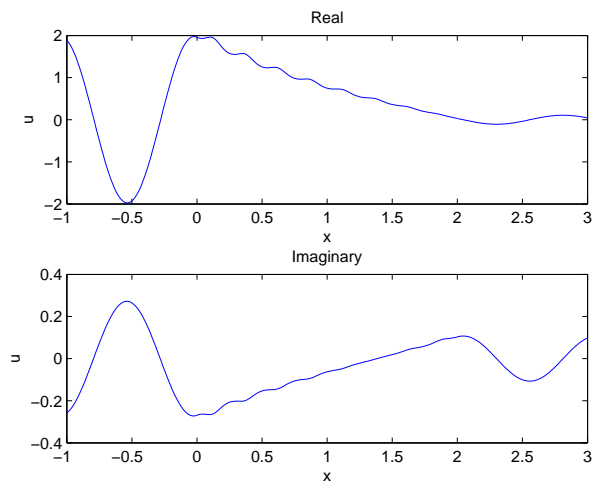
Figure 5.10: Real and imaginary plots of u over duct (2).
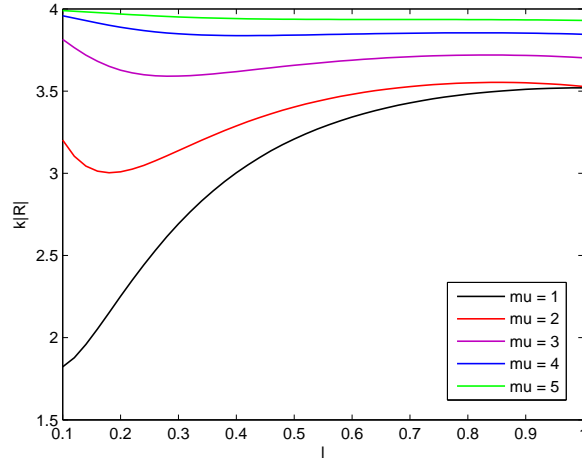
Figure 5.11: $k|R|$ against ℓ for duct (2) with different μ, where k is fixed ($k = 4$).
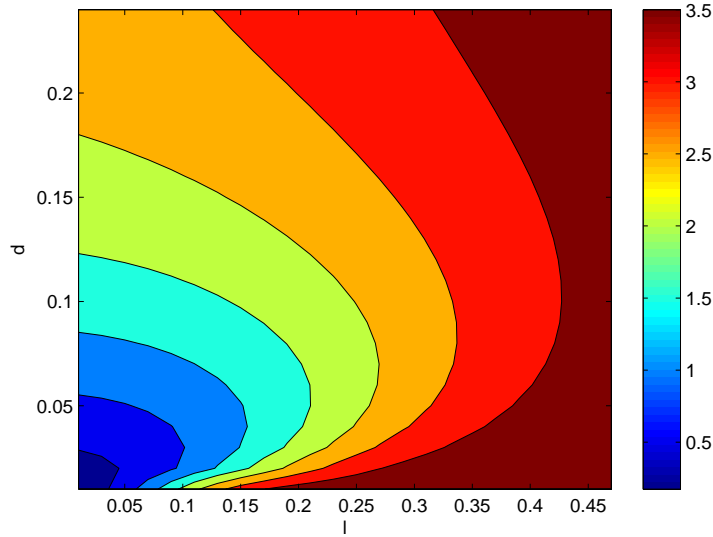
Figure 5.12: Contour plot of $k|R|$ for $\mu = 1$.
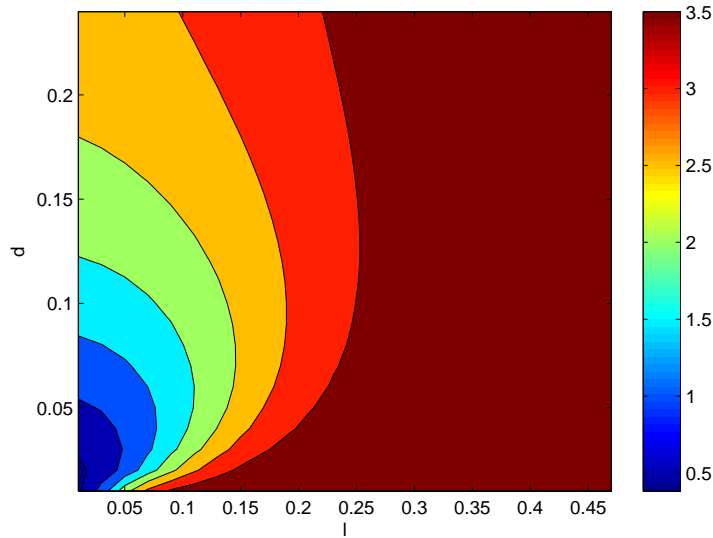
Figure 5.13: Contour plot of $k|R|$ for $\mu = 2$.

5.1.2 Multi-Mode Approximations

The obvious way to start this subsection is to compare some of the plots found with a single mode approximation to the plots created when using a multi-mode approximation. Figures (5.13) though to (5.18) do just this. When these figures are compared with their corresponding single mode approximations (figures (5.1) to (5.1.1) and (5.4) to (5.6)) there does not appear to be any significant differences. This is very promising as it means that when modelling acoustic wave transmission though a duct with Dirichlet boundary conditions along the walls of the duct, a single mode approximation is sufficient. To verify that this is true, figure(5.19) shows convergence after $N = 2$, and a difference smaller than 0.0001 prior to this. This figure portrays $|R|$ for varying N where $d = 0.1$, $\ell = 2$ and $\mu = 1$.
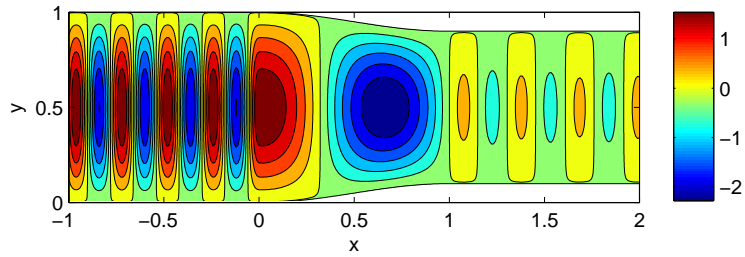
Figure 5.14: Contour plot of ϕ over duct (1) with $N = 10$.
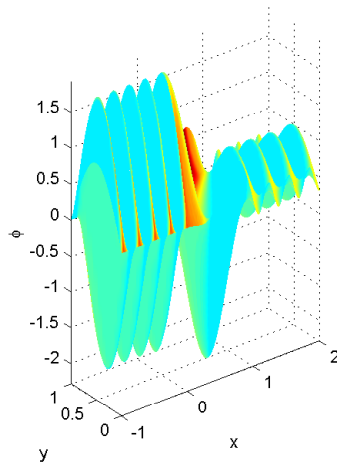
Figure 5.15: Surf plot of ϕ over duct (1) with $N = 10$.
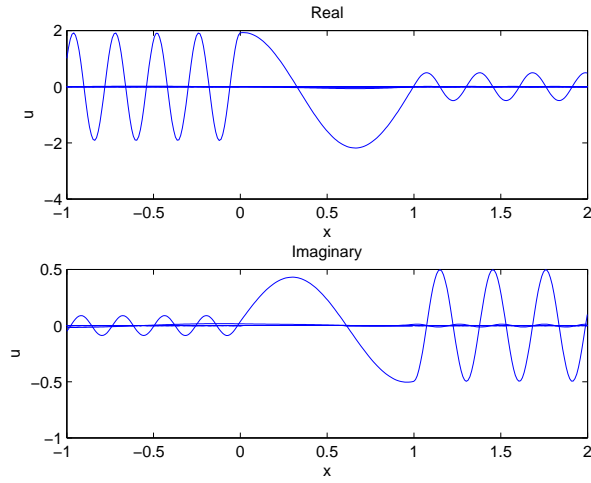
Figure 5.16: Real and imaginary plots of u over duct (1) with $N = 10$.
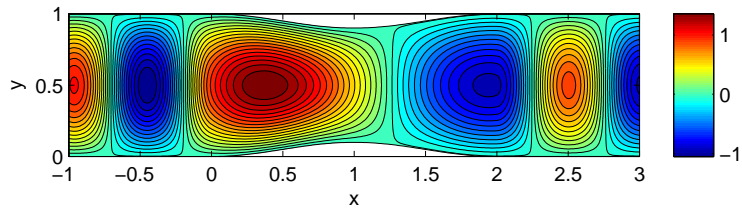
Figure 5.17: Contour plot of ϕ over duct (2) with $N = 10$.
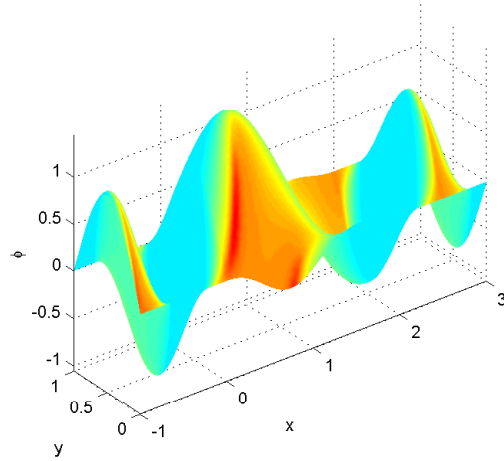
Figure 5.18: Surf plot of ϕ over duct (2) with $N = 10$.
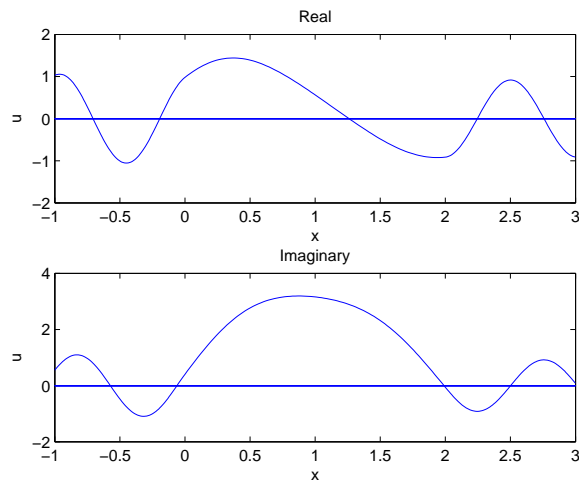
Figure 5.19: Real and imaginary plots of u over duct (2) with $N = 10$.

5.2   Trapped Wave Problem

5.2.1   Single Mode Approximation With $n = 1$

As mentioned in Section (3.2), before finding the velocity potential ϕ we must first find a value of k for which there is a trapped wave. Once again, we take duct (2)

$$a(x) = \begin{cases} 0 & x < 0 \\ d\sin^2\left(\frac{\mu\pi x}{\ell}\right) & 0 < x < \ell \\ 0 & x > \ell, \end{cases} \tag{5.5}$$

and

$$b(x) = \begin{cases} 1 & x < 0 \\ 1 - a(x) & 0 < x < \ell \\ 1 & x > \ell. \end{cases} \tag{5.6}$$

However, for this problem we shall choose $d = -0.15$. Let us first examine the duct with $\ell = 2$ and $\mu = 1$. Figure (5.20) shows the second boundary condition plotted against k. From this plot, it is difficult to determine whether there are any eigenvalues for this model, so figure (5.21) zooms in on a small section of the plot to verify that an eigenvalue exists. Using the bisection method, the root is found to be at $k = 2.8901$. This value of k is then to produce figures (5.22), (5.23) and (5.24), which show that the waves decay exponentially when outside of the undulating region. Most of the wave activity is restricted to the region $0 < x < \ell$ where the velocity potential ϕ reaches its peak at the center of the duct.

Figures (5.27), (5.28) and (5.29) are results produced from a similar duct. The values for ℓ and d remain the same, but $\mu = 2$ so we have each duct wall has two external humps. This new μ produces a new value of k, $k = 3.0501$. The figures show similar results to when $\mu = 1$, but the velocity potential ϕ decreases from the centre at a slower rate. Nonetheless, the waves decay exponentially in the uniform regions.
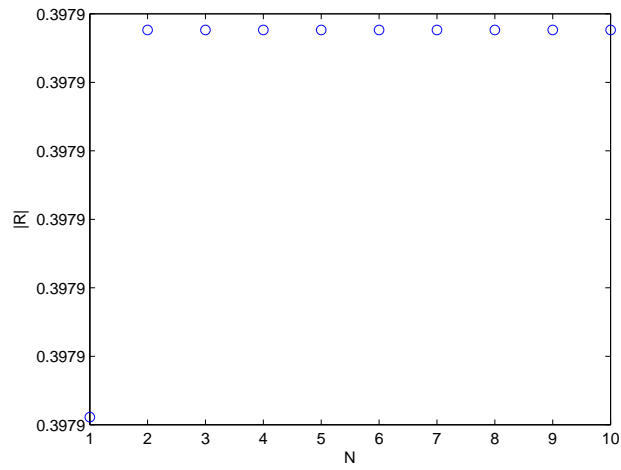
Figure 5.20: $|R|$ for varying N using duct(2).
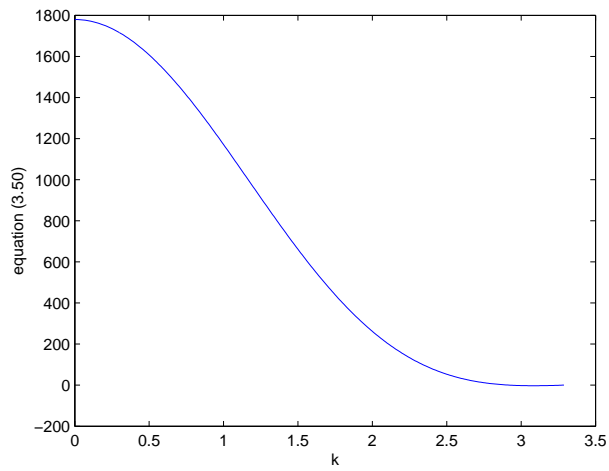
Figure 5.21: The second boundary condition (3.51) plotted against k using duct (2) for $\mu = 1$.
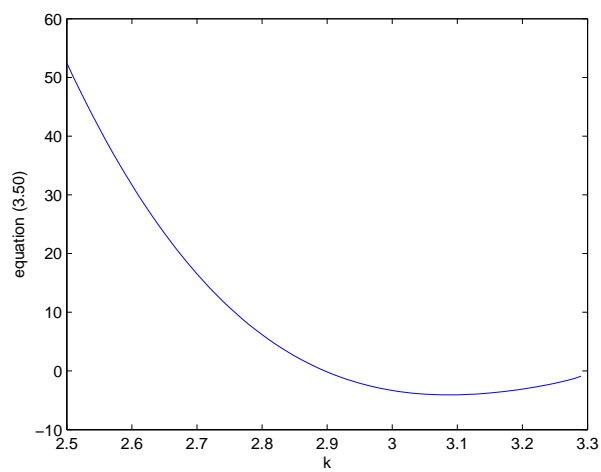
Figure 5.22: A close up of figure (5.20) to clearly see the that an eigenvalue exists.
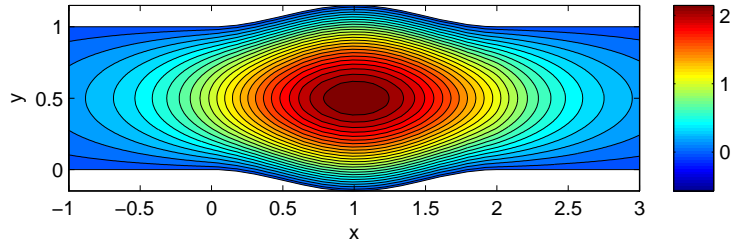
Figure 5.23: Contour plot of ϕ over duct (2) for $\mu = 1$.
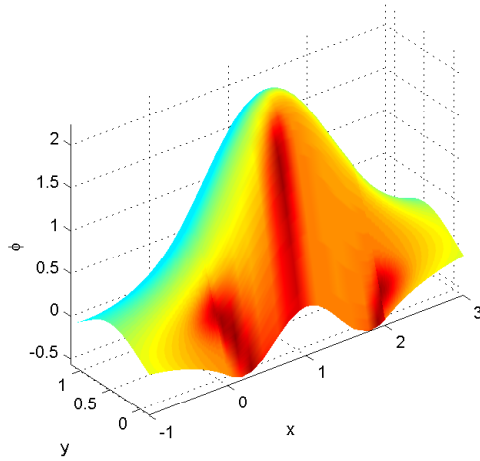
Figure 5.24: Surf plot of ϕ over duct (2) for $\mu = 1$.

44
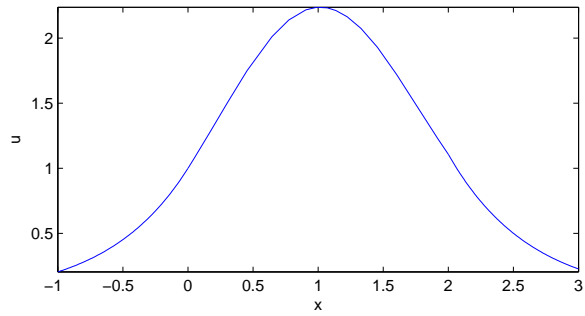
Figure 5.25: Real plot of u over duct (2) for $\mu = 1$.
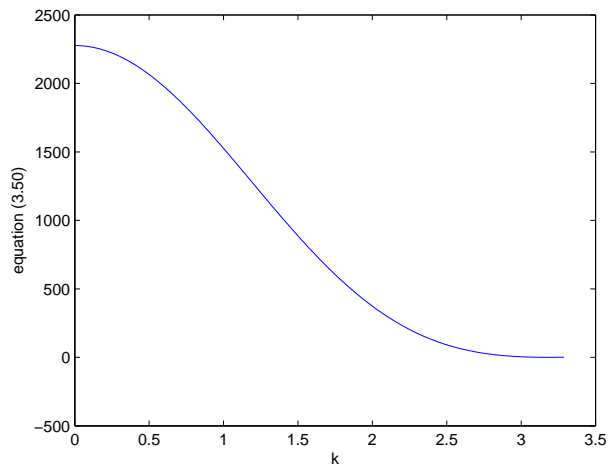
Figure 5.26: The second boundary condition (3.51) plotted against k using duct (2) for $\mu = 2$.
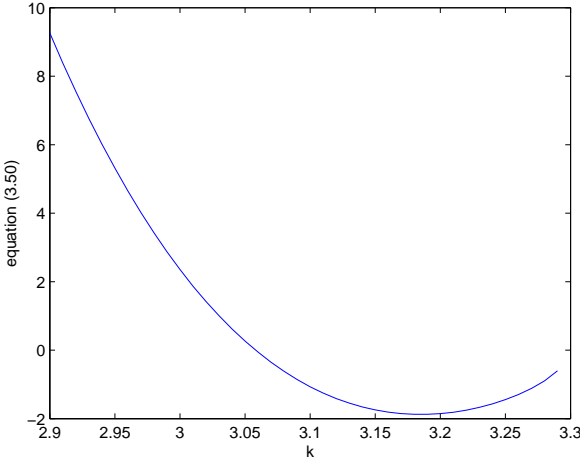
Figure 5.27: A close up of figure (5.25) to clearly see the that an eigenvalue exists.
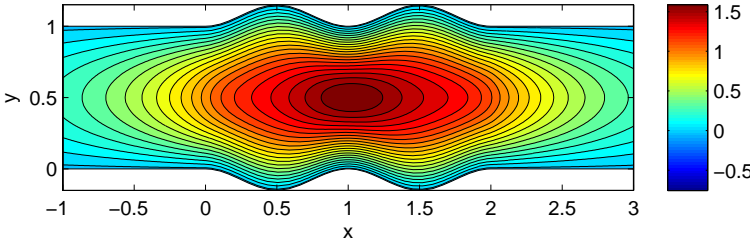
Figure 5.28: Contour plot of ϕ over duct (2) for $\mu = 2$.
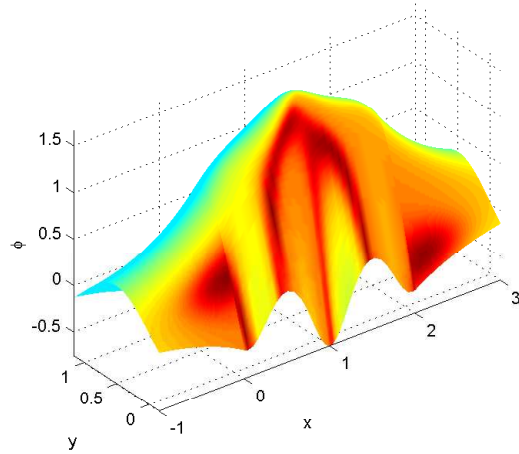
Figure 5.29: Surf plot of ϕ over duct (2) for $\mu = 2$.
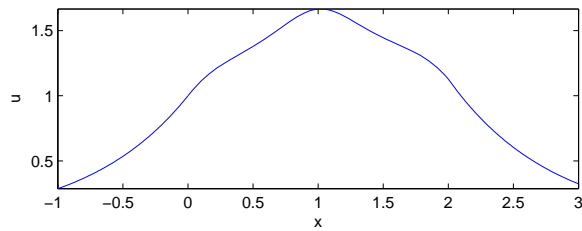
Figure 5.30: Real plot of u over duct (2) for $\mu = 1$.

47

5.2.2   Investigating Problems With More Than One Eigenvalue

Now suppose we have two or more trapped waves within the duct. For this to occur we require two or more eigenvalues. Whereas with the scattering problem we chose the first mode $n = 1$ to ensure that we have a propagating wave, this is not a restriction when modelling the trapped wave problem. As long as the waves in the uniform regions are evanescent, i.e $0 < k < \sqrt{\nu_n}$, we can choose n to be any integer when calculating $u(x)$ for these regions. Figures (5.30) and (5.31) show that as we choose larger n there are more eigenvalues, so there would be more trapped waves.

Figure (5.32) shows that for $n = 4$ there are three different trapped waves. These waves correspond to $k = 2.9601$, $k = 3.8101$ and $k = 4.6401$. Their separate plots are portrayed by figures (5.33) to (5.41). Although the different values of k produce very different results, all of them contain exponentially decaying waves within the uniform regions.

An interesting result here is found when the trapped waves for $n = 5$ are plotted. Figure (5.42) depicts four eigenvalues, and the bisection method find these to be $k = 3.1901$, $k = 3.8701$, $k = 4.8701$ and $k = 5.7601$. Now comparing the results from the first eigenvalue with the corresponding results for $n = 4$ we see that they have a similar shape. This is also the shape portrayed for when $n = 1$ in the Section 5.2.1. Now comparing the results from the second eigenvalues for both $n = 4$ and $n = 5$ we see that again, there is a similar shape. The velocity potential ϕ is at its highest to the left of the centre, and then reduces down to its lowest to the right. For the third eigenvalue, and for both n, the plots depict two equal peaks for ϕ either side of a trough in the centre of the duct. Lastly, the fourth eigenvalue for $n = 5$ produces a more complex shape. The velocity potential appears to oscillate though the varying region before decaying exponentially in the varying regions.

It would appear that as n increases and creates more eigenvalues, the plots relating to the corresponding eigenvalues for different n are the same. As the eigenvalue gets larger the trapped wave oscillates more in $0 < x < \ell$. These results do not prove that this is true for all n, merely for the examples we have modelled here.
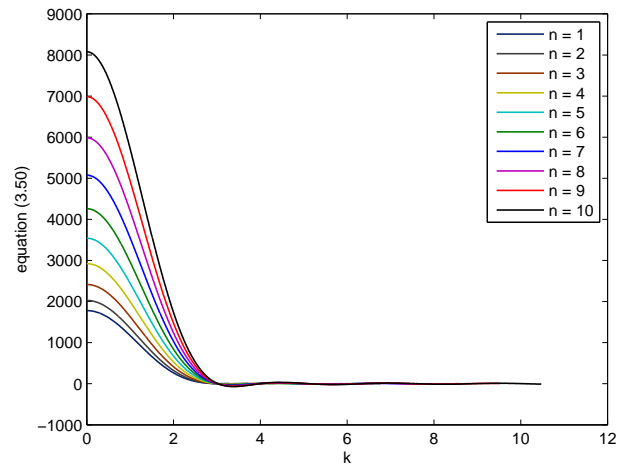
Figure 5.31: The second boundary condition (3.51) plotted against k using duct (2) for varying n.
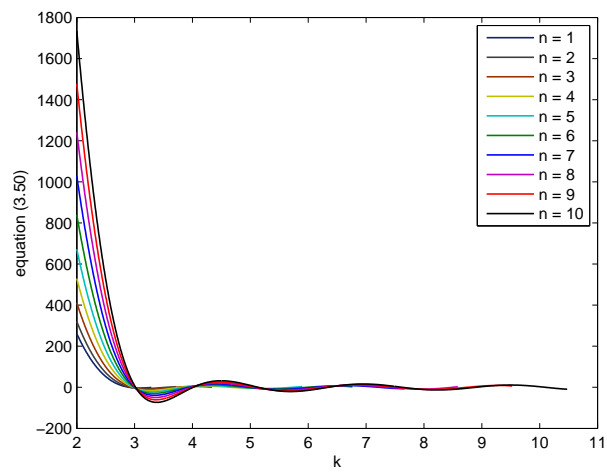
Figure 5.32: A close up of figure (5.30).
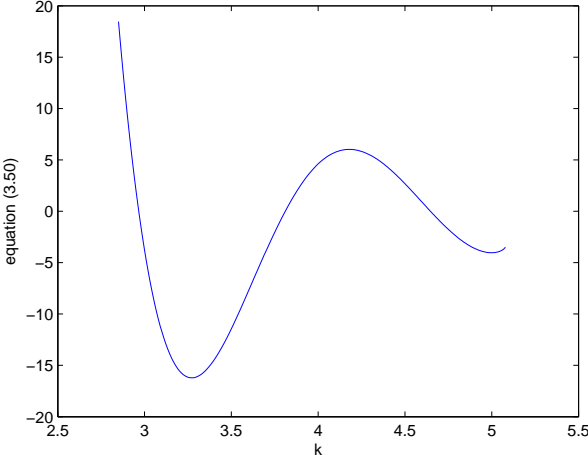
Figure 5.33: A close up of the second boundary condition (3.51) plotted against k to clearly see how many eigenvalues exists for $n = 4$.
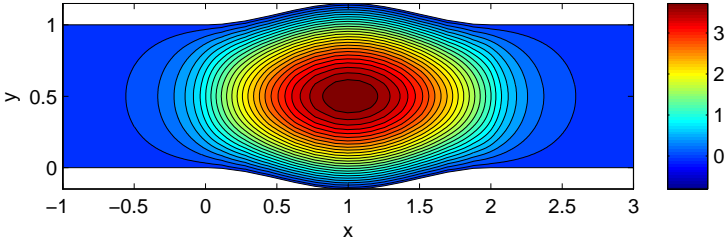
Figure 5.34: Contour plot of ϕ over duct (2) for the first trapped wave ($n = 4$).
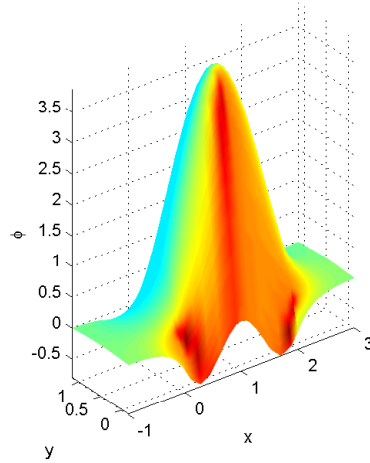
Figure 5.35: Surf plot of ϕ over duct (2) for the first trapped wave ($n = 4$).
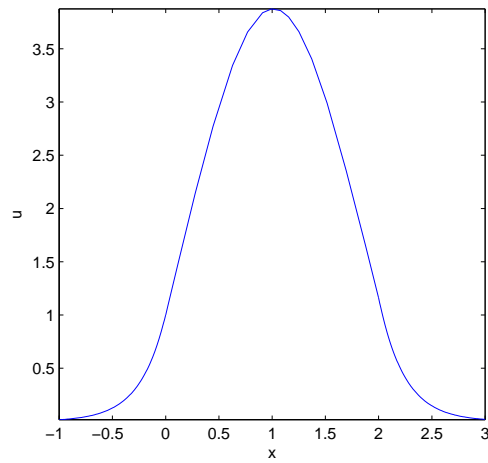
Figure 5.36: Real plot of u over duct (2) for the first trapped wave ($n = 4$).
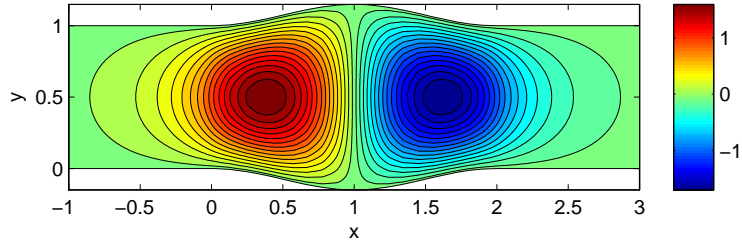
Figure 5.37: Contour plot of ϕ over duct (2) for the second trapped wave $(n = 4)$.
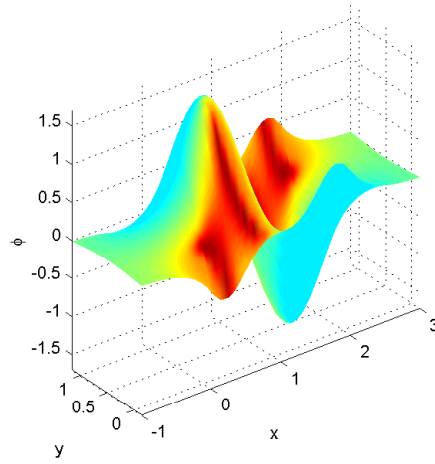
Figure 5.38: Surf plot of ϕ over duct (2) for the second trapped wave $(n = 4)$.
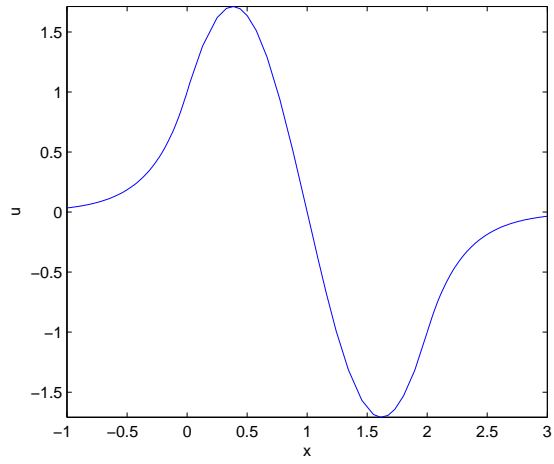
Figure 5.39: Real plot of u over duct (2) for the second trapped wave ($n = 4$).
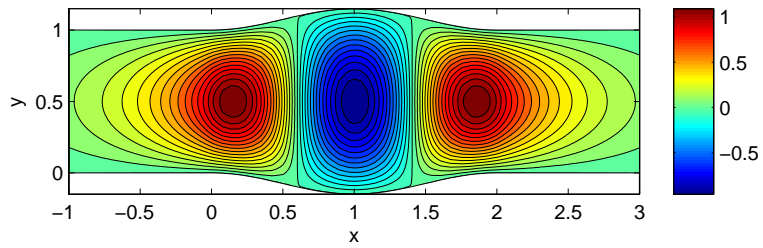
Figure 5.40: Contour plot of ϕ over duct (2) for the third trapped wave ($n = 4$).
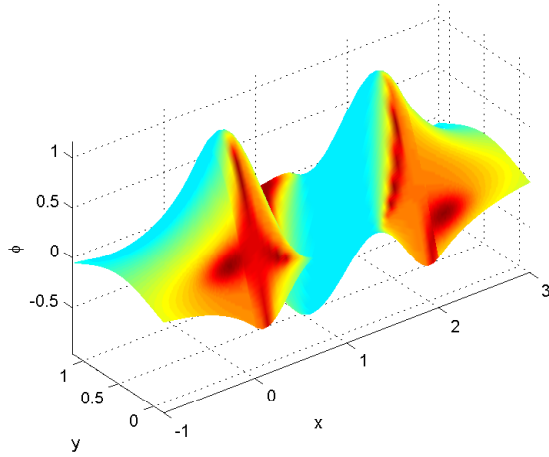
Figure 5.41: Surf plot of ϕ over duct (2) for the third trapped wave ($n = 4$).
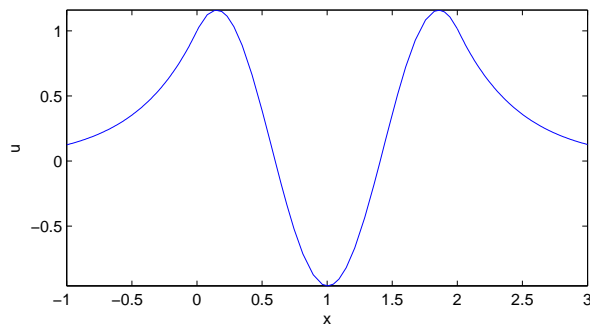
Figure 5.42: Real plot of u over duct (2) for the third trapped wave ($n = 4$).
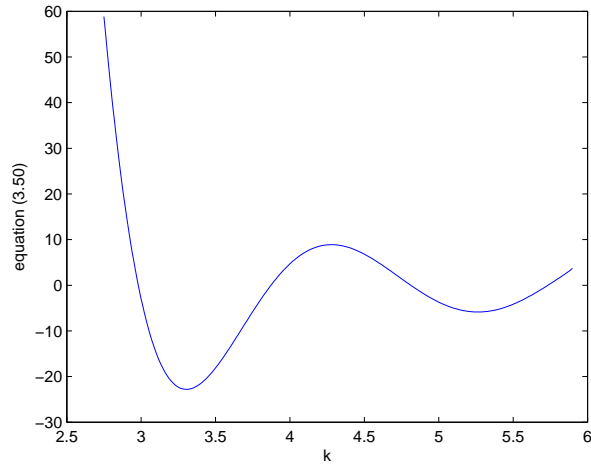
Figure 5.43: A close up of the second boundary condition (3.51) plotted against k to clearly see how many eigenvalues exists for $n = 5$.
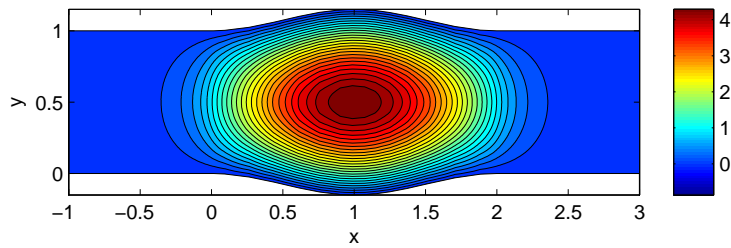
Figure 5.44: Contour plot of ϕ over duct (2) for the first trapped wave ($n = 5$).
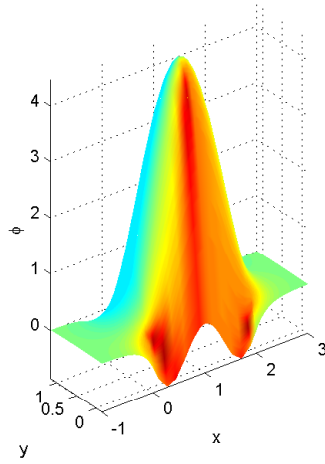
Figure 5.45: Surf plot of ϕ over duct (2) for the first trapped wave ($n = 5$).
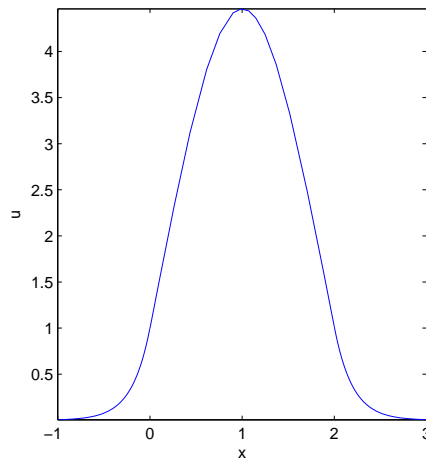
Figure 5.46: Real plot of u over duct (2) for the first trapped wave ($n = 5$).
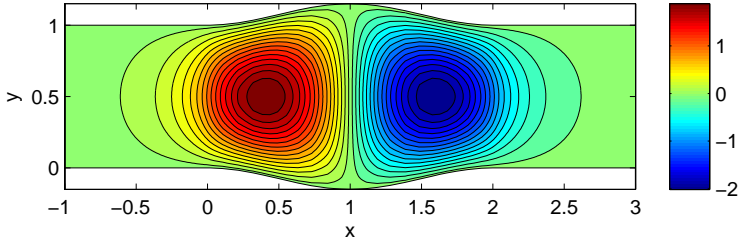
Figure 5.47: Contour plot of ϕ over duct (2) for the second trapped wave ($n = 5$).
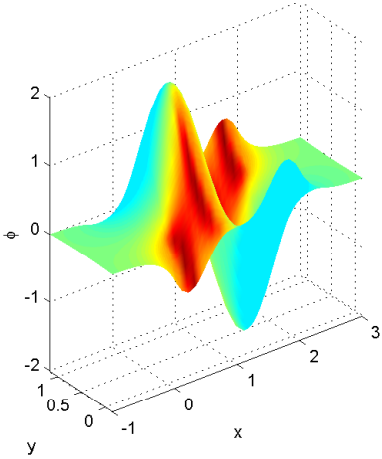
Figure 5.48: Surf plot of ϕ over duct (2) for the second trapped wave ($n = 5$).
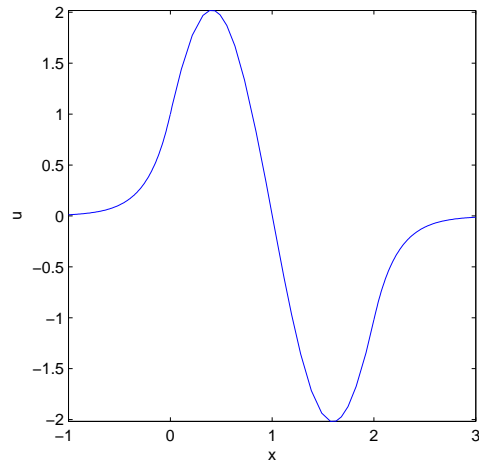
Figure 5.49: Real plot of u over duct (2) for the second trapped wave ($n = 5$).
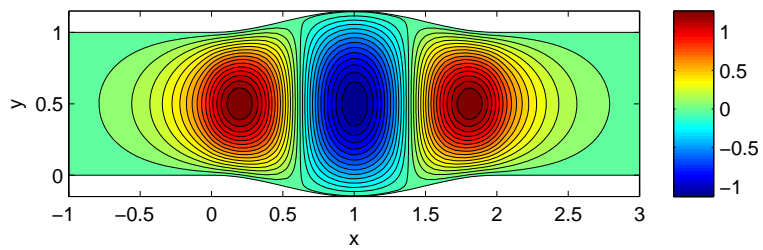
Figure 5.50: Contour plot of ϕ over duct (2) for the third trapped wave ($n = 5$).
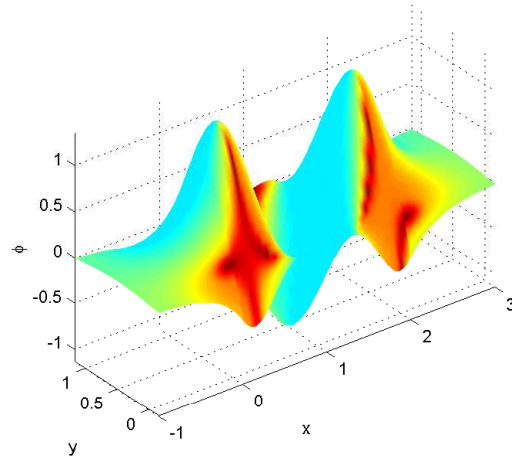
Figure 5.51: Surf plot of ϕ over duct (2) for the third trapped wave ($n = 5$).
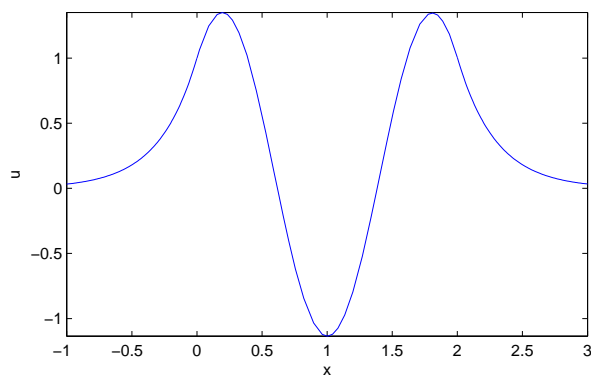
Figure 5.52: Real plot of u over duct (2) for the third trapped wave ($n = 5$).
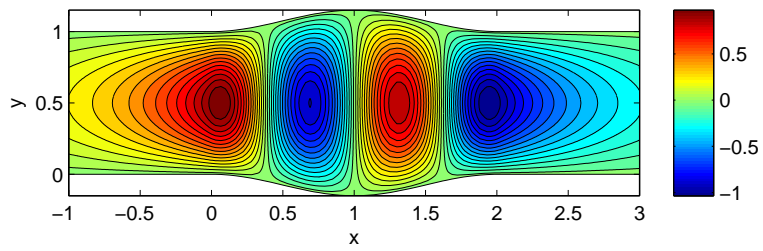
Figure 5.53: Contour plot of ϕ over duct (2) for the fourth trapped wave ($n = 5$).
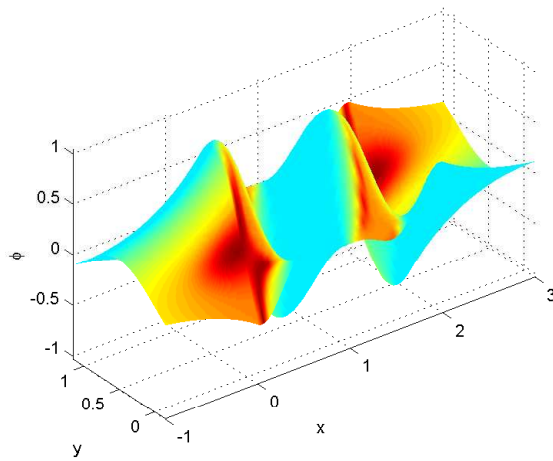
Figure 5.54: Surf plot of ϕ over duct (2) for the fourth trapped wave ($n = 5$).
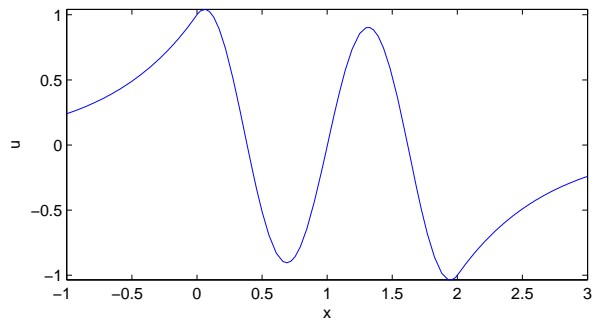
Figure 5.55: Real plot of u over duct (2) for the fourth trapped wave ($n = 5$).

Chapter 6

Further Work

Two areas of possible further work are multi-mode approximations for the trapped wave problem, and exploring the effect of Neumann boundary conditions on the top and bottom of the duct. Let us begin with the former.

6.1 Multi-Mode Approximations For The Trapped Wave Problem

When modelling a trapped wave problem with a single mode approximation, we had to find an eigenvalue first. We then set k to equal the eigenvalue so as to produce a trapped wave within the duct. We found the eigenvalue by plotting the second boundary condition (3.51) against k and used the bisection method to find the root. Now, we saw from Chapter 4 that multi-mode approximations produced N ODEs and $2N$ boundary conditions. This makes the eigenvalue problem much more complicated. Rather than seeking where one function crosses the x - axis, we would be seeking the point (or points) where N functions cross the x-axis at the same point (or points).

6.2 Neumann Boundary Conditions Along Duct Walls

So far, we have only worked with Dirichlet boundary conditions on the top and bottom of the duct. Now let us suppose we had Neumann conditions. If we recall, in Section 3.1 we separated the variables of ϕ in regions of constant width. Applying the Dirichlet boundary conditions in the y direction of the

separated solution gave us (3.8),

$$Y_n(y) = \sin\left(\frac{n\pi(y - a_j)}{b_j - a_j}\right), \qquad j = 0, 1 \text{ and } n = 1, 2, ...,$$

which ensured $y(a_j) = y(b_j) =$, where $j = 0, 1$. For Neumann boundary conditions we require the x derivatives of y to be zero, $y'(a_j) = y'(b_j) = 0$, meaning

$$Y_n(y) = \cos\left(\frac{n\pi(y - a_j)}{b_j - a_j}\right), \qquad j = 0, 1 \text{ and } n = 1, 2, ...$$

Modelling a duct with Neumann boundary conditions can be awkward because we require the normal derivative to always be orthogonal to the duct walls. This is straightforward in the uniform sections as the normal is simply in the y direction. However, for the undulating regions it is less manageable. The normal in the varying section changes with the duct wall and is often not in the y direction. Nonetheless, when modelling Neumann boundary conditions we assume that the normal is in the y direction for the whole duct. This assumption produces results that seem reasonable for most of the duct - within the uniform regions the waves coincide with the duct walls at a right angle. However, in the the undulating region the waves behave reasonably when they are not close to the duct walls - but when they are close to the wall they change direction so that they coincide with the duct wall vertically.

6.3   Related Work

Hazard and Luneville (2002) also modelled a duct with two uniform regions either side of an undulating region. They then choose k and the width of the duct so that exactly two modes propagate. A single mode is then sent in from the left so that only two modes leave the duct from the right, meaning the undulating region of the duct moves all the inserted energy into two modes. To achieve this result the duct shape is chosen carefully by setting up a minimisation problem. For example, the choice of coefficients in a truncated Fourier series representation of the duct walls could be tuned to minimise the amount of outgoing waves. They managed to determine duct walls so that over ninety-nine percent of the incoming energy is transferred to two outgoing modes.

Chapter 7

Summary and Conclusions

This dissertation has used methods of approximating scattering over a varying water-bed to model acoustic wave transmission through ducts. We started by becoming familiar with the water wave problem and learning one method that can be used to derive the mild-slope equation, and the modified mild-slope equation. We then adapted this method to produce a system of ordinary differential equations (ODEs) in terms of $u_n(x)$, for x within the varying region of the duct $(0 < x < \ell)$. We begin with only taking a single mode approximation meaning we only have one ODE.

For the scattering problem, when examing the regions of constant width, we can use separation of variables. The separated solution in the y direction, along with restrictions determined due to Dirichlet boundary conditions on the top and bottom of the duct, enable us to determine $Y_n(y)$. Now, the separated solution in the x direction provides us with a general solution for $u_1(x)$ in the uniform domains. By assuming the undulating duct walls meet the uniform regions smoothly, we use the solutions for u_1 in the uniform regions to determine the boundary conditions for our ODE. The dissertation discusses how to manipulate the problem so we can use the built-in Matlab function `bvp4c` to find a solution for u_1 in the undulating region. Once the boundary value problem is solved, it is simply a matter of substitution to find the exact solutions in the two uniform regions. Once u_1 and Y_1 have been calculated, it is a straightforward multiplication to define the velocity potential ϕ over the whole duct.

When solving the scattering problem with more than one mode, it is approached in a similar fashion to the single mode approximation. We continue to use `bvp4c` however, as there would be a system of ODEs and several boundary conditions either side of the undulating domain, we create additional function handles to store all the coefficients in matrices and vectors. The system of

equations is then solved in a manner that is parallel to the single mode approximation, thus allowing us to find ϕ.

For a single mode approximation, we did not only explore the scattering problem, but also the trapped wave problem . This problem involved an additional step before being able to find u_1 as it is an eigenvalue problem. So firstly, we had to discover a situation that would provide us with a trapped wave. To find an approximation to the trapped wave problem, another Matlab programme was discussed - `ode23`. The required manipulation of our ODE and the boundary conditions to find an eigenvalue was more subtle for this problem than for the scattering problem.

Next, we saw the numerical results of the mentioned models. The results for the multi-mode approximations are almost the same as the single mode approximations. This indicates, that for a scattering problem with Dirichlet conditions along the duct walls, a single mode approximation is efficient. As the single mode approximation does not require matrices of coefficients to be stored, it is definitely the more cost-efficient of the two approximations. However, as discussed in Chapter 6, it is more challenging to exactly satisfy Neumann boundary conditions. When modelling a duct with Neumann conditions along the duct walls, additional modes may have a more obvious purpose.

The numerical results for the trapped wave problem showed that when we chose $n = 1$ as our single mode, we had one trapped wave within the duct. When we chose larger n we obtained more trapped waves. For a particular n, as the eigenvalues k increased so did the number of oscillations within the undulating region. Regardless of the value of n and the wave activity within the varying region, the waves would always decay exponentially in the uniform regions as expected.

Lastly, we finished with a mention of areas for further work. This included looking at modelling the trapped wave problem with a multi-mode approximation, and the effect this would have when solving the eigenvalue problem. We also considered how we would model a duct with Neumann boundary conditions and the results we would achieve. We ended this chapter with a mention of related work by Hazard and Luneville (2002).

Bibliography

[1] J. C. W. Berkhoff, Computation of combined refraction-diffraction. *Proc. 13th Intl Conf. on Coastal Engng, July 1972, Vancouver, Canada* **471-490** (1973)

[2] J. C. W. Berkhoff, Mathematical models for simple harmonic linear water waves. Wave diffraction and refraction. *Delft. Hydr. Rep.* **154-IV** (1976)

[3] P. G. Chamberlain, and D. Porter, Linear wave scattering by two-dimensional topography. In Gravity Waves in Water of Finite Depth, Ed. J.N.Hunt, Computational Mechanics, 13 - 53, 1997

[4] P. G. Chamberlain, and D. Porter, Wave scattering over uneven depth using the mild-slope equation. *Wave Motion* **267-285** (1993)

[5] P. G. Chamberlain, and D. Porter, The modified mild-slope equation. *J. Fluid Mechanics* **393-407** (1995)

[6] P. G. Chamberlain, and D. Porter, Multi-mode approximations to wave scattering by an uneven bed. *J. Fluid Mechanics*, 556 **421-441** (2006)

[7] S. Chidlow, Approximations to linear wave scattering by topography using an integral equation approach. *Univ. of Reading* (2005)

[8] J. T. Kirby, A general wave equation for waves over rippled beds. *J. Fluid Mechanics*, 162 **171-186** (1986)

[9] C. Hazard. and E. Luneville, An improved multimodal approach for non-uniform acoustic waveguides. *IMA Journal of App. Mathematics*

[10] C. Hazard. and E. Luneville, Multimodal approach and optimum design in non uniform waveguides. *Journees Europeennes sur les Methodes Numeriques en Electromagnetisme* (2002)

[11] S. R. Massel, Extended refraction-diffraction equation for surface waves. *Coastal Engng*, 19 **97-126** (1993)

[12] D. Porter and D. J. Staziker Extensions of the mild-slope equation. *J. Fluid Mechanics*, 300 **367-382** (1995)

[13] D. Porter , The mild-slope equations. *J. Fluid Mechanics*,494 **51-63** (2003)

[14] R. Pratap, Getting started with Matlab 7. A quick Introduction for scientists and engineers. *Oxford University Press, New York* (2006)

[15] L. F. Shampine, J. Kierzenka and M. W. Reichelt, Solving boundary value problems for ordinary differential equations in Matlab using bvp4c. **142-147**(2006)

[16] R. Smith and T. Sprinks, Scattering of surfaces waves by a conical island. *J. Fluid Mechanics*,72 **373-384** (1975)

[17] http://en.wikipedia.org/wiki/Bisection_method